RESEARCH ARTICLE VOLCANICA

Assessing the effectiveness of low-cost air quality monitors for identifying volcanic SO_2 and PM downwind from Masaya volcano, Nicaragua

Rachel C. W. Whitty[*α], Melissa A. Pfeffer[β], Evgenia Ilyinskaya[α], Tjarda J. Roberts[γ], Anja Schmidt[δ,ϵ], Sara Barsotti[β], Wilfried Strauch[ζ], Leigh R. Crilley[η], Francis D. Pope[θ], Harold Bellanger[ι], Elvis Mendoza[ζ], Tamsin A. Mather[κ], Emma J. Liu[λ], Nial Peters[μ], Isabelle A. Taylor[ν], Hilary Francis[ξ], Xochilt Hernández Leiva[†o], Dave Lynch[π], Sébastien Nobert[ι,ρ], Peter Baxter[ς]

[α] *Institute of Geophysics and Tectonics, School of Earth and Environment, University of Leeds, Leeds, United Kingdom.*
[*] *Full list of affiliations given in Affiliations section.*

Abstract

Gas and particulate matter (PM) emissions from Masaya volcano, Nicaragua, cause substantial regional volcanic air pollution (VAP). We evaluate the suitability of low-cost SO_2 and PM sensors for a continuous air-quality network. The network was deployed for six months in five populated areas (4–16 km from crater). The SO_2 sensors failed and recorded erroneous values on multiple occasions, likely due to corrosion, requiring significant maintenance commitment. The PM sensors were found to be robust but data required correction for humidity. SO_2 measurements could not be used as stand-alone tools to detect occurrence of VAP episodes (VAPE), but an SO_2/PM correlation reliably achieved this at near-field stations, as confirmed by meteorological forecasts and satellite imagery. Above-background PM concentrations reliably identified VAPE at both near-field and far-field stations. We suggest that a continuous network can be built from a combination of low-cost PM and SO_2 sensors with a greater number of PM-only sensors.

Resumen

Las emisiones de gases y partículas (PM) del volcán Masaya, Nicaragua, causan una importante contaminación atmosférica volcánica regional (VAP). Evaluamos la idoneidad de los sensores de SO_2 y PM de bajo coste para una red continua de calidad del aire. La red se desplegó durante seis meses en cinco zonas pobladas (a 4–16 km del cráter). Los sensores de SO_2 fallaron y registraron valores erróneos en múltiples ocasiones, probablemente debido a la corrosión, lo que requirió un importante compromiso de mantenimiento. Los sensores de PM resultaron ser robustos, pero los datos requerían una corrección en función de la humedad. Las mediciones de SO_2 no pudieron utilizarse como herramientas independientes para detectar la aparición de episodios de VAP (VAPE), pero una correlación SO_2/PM lo consiguió de forma fiable en las estaciones cercanas, como confirmaron las previsiones meteorológicas y las imágenes por satélite. Las concentraciones de PM por encima del fondo identificaron de forma fiable los VAPE tanto en las estaciones de campo cercano como en las de campo lejano. Sugerimos que se puede construir una red continua a partir de una combinación de sensores de PM y SO_2 de bajo coste con un mayor número de sensores sólo de PM.

Keywords: `SO2; PM; Masaya; Volcano; Low-cost; Air-quality;`

1 Introduction

Masaya is an active basalt volcanic complex in Nicaragua, Central America. It has a near-continuous history of pit crater formation, sporadic lava lake activity, and degassing as far back as, at least, the 1500s [Rymer et al. 1998]. Santiago pit crater, initially formed around 1858–1859 [McBirney 1956], is the location of current volcanic activity and has undergone five periods of lava lake development and multiple phases of gas crisis with intense degassing activity [McBirney 1956; Stoiber et al. 1986]. The latest and current outgassing crisis started in 1993 and has resulted in large fluxes of volcanic gas into the atmosphere [Rymer et al. 1998; Burton et al. 2000; Williams-Jones et al. 2003; Mather et al. 2006a] with sulphur dioxide (SO_2) flux ranging from 120 to 2680 metric tons per day (Figure 1).

[*] Corresponding author: eercww@leeds.ac.uk
[†] Formerly at Universidad Americana, Managua, Nicaragua; formerly at Faculty of Education, University of Cambridge, Cambridge, United Kingdom.

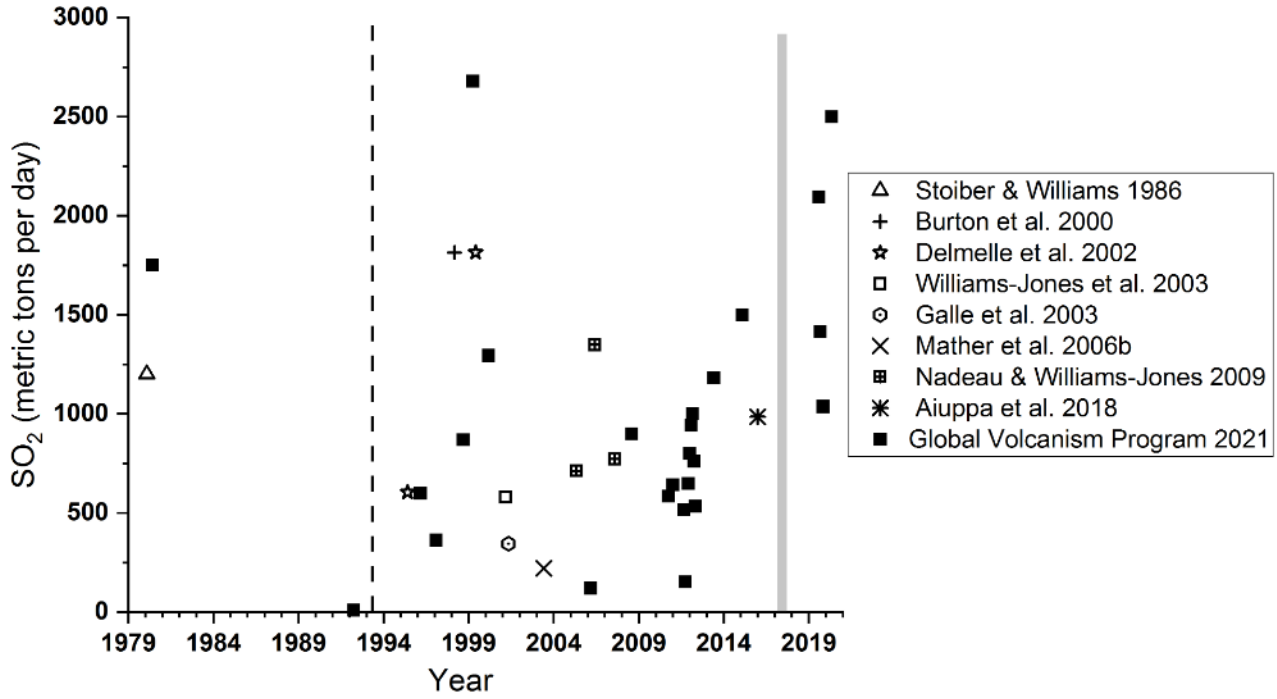

Figure 1: SO_2 emissions from Santiago crater, Masaya volcano, from 1979 to 2020. Black dashed line indicates initiation of gas crisis in May 1993. Grey shaded area indicates the AQMesh downwind measurement period (this study) from February to August 2017. SO_2 emissions data sourced from Stoiber et al. [1986], Burton et al. [2000], Delmelle et al. [2002], Galle et al. [2003], Williams-Jones et al. [2003], Mather et al. [2006b], Nadeau and Williams-Jones [2009], Aiuppa et al. [2018], and Global Volcanism Program [2021].

Masaya volcano has a subdued topography, situated at 635 metres above sea level (m asl), and this often results in the volcanic plume remaining in the atmospheric boundary layer [Delmelle et al. 2002]. The injection of the plume into the low atmosphere means that the plume can "ground", causing exposure of the land-surface to high concentrations of toxic gas and aerosols. Prevailing easterly winds mean the plume is commonly moved towards the Las Sierras highlands, an area higher (925 m asl) than the crater summit, causing damage to vegetation (including cultivated crops), machinery and buildings over a large area downwind of the crater [Baxter et al. 1982; Delmelle et al. 1999; van Manen 2014; Williams-Jones and Rymer 2015]. Volcanic plumes that remain in the lower atmosphere, such as that emitted from Masaya volcano, are commonly composed of a complex and chemically-evolving mixture of both volcanic and atmospheric gases as well as primary and secondary aerosol particles, dust, and ash [Pfeffer et al. 2006b; Oppenheimer and McGonigle 2009; von Glasow et al. 2009; Langmann 2014; Mason et al. 2021]. Volcanic emissions released into the lower atmosphere can have a large impact on air quality, the environment, and human and animal health across local to regional areas [Mather 2015; Schmidt et al. 2015; Tam et al. 2016; Ilyinskaya et al. 2017; Whitty et al. 2020; Carlsen et al. 2021b; Ilyinskaya et al. 2021].

SO_2 is often the focal point of gas emission monitoring at volcanoes due to its high concentration in volcanic plumes relative to the background ambient atmosphere, as well as its well-recognised environmental and air quality impacts [Cadle et al. 1971; Lambert et al. 1988; Loughlin et al. 2012; Schmidt et al. 2015]. Methods to monitor volcanic SO_2 emissions include remote sensing approaches (that enable determination of gas flux) and *in situ* methods such as Multi-Gas instruments that contain electrochemical sensors for SO_2 detection. Studies using Multi-Gas have mostly focused on the near-source near-summit plume, detecting SO_2 at up to tens or even hundreds of parts per million volume (ppmv) [Shinohara et al. 2008; Roberts et al. 2012; Aiuppa et al. 2018]. While the principal of SO_2 measurements is the same (electrochemical sensors), the concentration range in downwind areas is several orders of magnitude lower than near-source and therefore presents different challenges for detection accuracy. Measurement of volcanic SO_2 at sub-ppmv levels has also been demonstrated using electrochemical sensors [Hagan et al. 2018; Roberts et al. 2018]. In a recent study, networks of low-cost SO_2 and particle sensors have been used to monitor volcanic pollution from the 2018 eruption of Kīlauea (USA) [Crawford et al. 2021].

Exposure to SO_2 can result in irritation and inflammation of the eyes and the upper respiratory tract [Pohl 1998; Miller 2004; Longo et al. 2008]. Population sub-groups including asthmatics, children, and

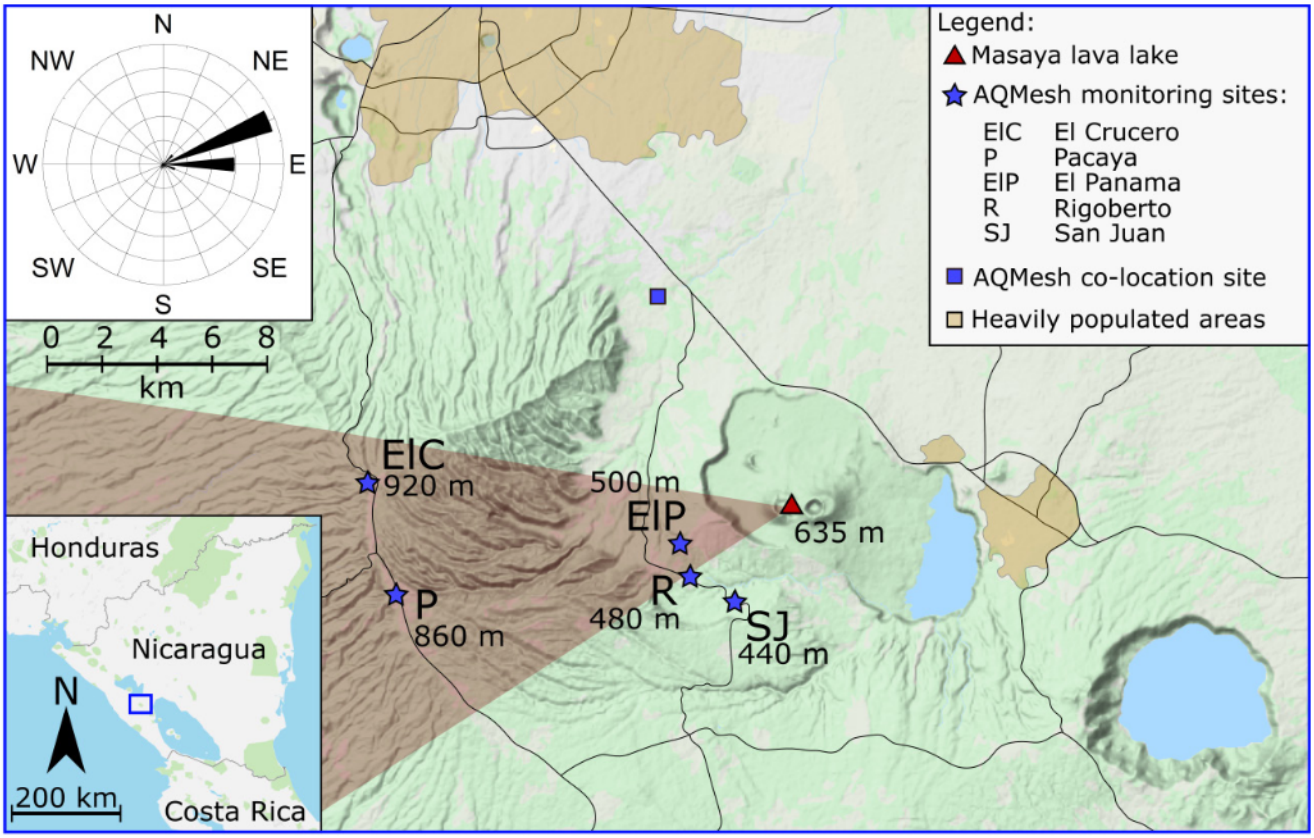

Figure 2: Topographic map of Masaya volcano and the AQMesh sampling stations with heights in metres above sea level (asl) for sampling stations and Masaya's Santiago Crater. Upper left inset indicates the wind rose referring to 948 metres asl for the period February to August 2017, data derived from ECMWF forecast meteorological data. The red shaded area indicates prevailing plume dispersion, graphically presented from the most frequent (76 %) wind direction derived from ECMWF data at 948 metres asl. Lower left inset indicates geographical position of Masaya volcano. Base topographic map from Krogh [2019].

respiratory- or cardiac-compromised individuals are particularly vulnerable to exposure to SO_2 [ATSDR 1998; CRI 2004].

Once in the atmosphere, SO_2 is affected by chemical and physical processes, including gas-phase reactions and reactions with liquid and solid suspended particles, leading to conversion of SO_2 to sulphate aerosols [Stockwell and Calvert 1983; Allen et al. 2002; Delmelle et al. 2002]. The lifetime of SO_2 in the troposphere is usually considered to be in the range of days to a week [Allen et al. 2002; Rotstayn and Lohmann 2002; Pfeffer et al. 2006a; Pattantyus et al. 2018], with the rate of SO_2 conversion depending on the relative humidity, temperature, interactions with clouds, and the availability of oxidants [Saxena and Seigneur 1987; Oppenheimer et al. 1998]. Through a number of reaction pathways (including oxidation with the hydroxyl radical, OH, and with hydrogen peroxide, H_2O_2, and ozone, O_3), SO_2 is gradually converted to sulphate aerosol, H_2SO_4, [Stockwell and Calvert 1983; Allen et al. 2002], which is a dominant component of volcanic particulate matter (PM) [Tam et al. 2016; Pattantyus et al. 2018].

Volcanic PM can be monitored *in situ* in real-time by deploying devices designed to measure atmospheric PM such as optical particle counters and other PM instruments [Mather et al. 2003; Allen et al. 2006; Ilyinskaya et al. 2010; Roberts et al. 2018; Whitty et al. 2020]. PM is commonly sub-divided into size categories of PM_1, $PM_{2.5}$, and PM_{10} (PM with particle diameters <1 µm, <2.5 µm and <10 µm, respectively). This categorisation into cumulative size modes is important because particles of different sizes can have varying health impacts, with smaller particles having a larger relative surface area for the absorption of toxic chemicals as well as a greater efficiency at physical translocation from the respiratory tract to other areas of the body [Schlesinger et al. 2006]. For example, exposure to fine particulates in the $PM_{2.5}$ size category has been found to cause 3 % of global mortality from cardiopulmonary disease and 5 % mortality from cancer of the bronchus, lung, and trachea [Cohen et al. 2005]. Recent studies have also investigated a link between exposure to PM and decline in short-term cognitive abilities [Shehab and Pope 2019; Gao et al. 2021]. The chemical composition of volcanic PM is heterogeneous, with common chemical species including sulphates (primary emissions or formed via oxidation of

sulphur gases) [Cadle et al. 1971; Stockwell and Calvert 1983; Allen et al. 2002; Mather et al. 2003; Langmann 2014] and halides, with an array of metals and metalloids including environmentally-harmful species such as lead and cadmium [Longo 2013; Langmann 2014; Ilyinskaya et al. 2017; 2021; Mason et al. 2021]. Volcanic PM may also include particles mixed in from the background atmosphere derived from sources such as sea spray, industrial and transport sources, ambient matter, and fine wind-blown mineral dust [Lim et al. 2012; Tam et al. 2016; Holgate 2017; Butwin et al. 2019]. Exposure to H_2SO_4, a dominant component of volcanic PM [Mather et al. 2006b; Ilyinskaya et al. 2017; Mason et al. 2021], can result in irritation of the eyes and respiratory tract [Schlesinger 1985; Williams-Jones and Rymer 2015; Carlsen et al. 2021a].

The persistent SO_2 and PM-rich volcanic plume emitted from Masaya volcano has led to long-term contamination and fumigation of an area >1200 km^2 downwind of the volcano following the prevailing wind direction [Delmelle et al. 2002; Williams-Jones and Rymer 2015]. A study by Delmelle et al. [2002] using time-averaged samplers found background concentrations of SO_2 <2 ppbv (parts per billion by volume) to the east of Masaya volcano in upwind locations in 1998 and 1999. The highest SO_2 levels were measured in the fumigated area to the west in the area within 4 km of Masaya volcano, with concentrations of up to 230 ppbv coinciding with descriptions of the local vegetation as "devastated" [Delmelle et al. 2002]. Average SO_2 concentrations in the Las Sierras highlands were ~100 ppbv in 1999 [Delmelle et al. 2002]. In 2010, the U.S. Environmental Protection Agency (EPA) set the National Ambient Air Quality Standard (NAAQS) for SO_2 mass concentration exposure limits at 75 ppbv as a 1-hour average [EPA 2010]. As well as impacting the local vegetation, Masaya's volcanic plume interacts strongly with metal structures, particularly the roofs of buildings, which consistently have to be replaced or painted every six months due to rapid corrosion [Baxter et al. 1982; Delmelle et al. 2002; van Manen 2014].

Volcanic activity at Masaya volcano is monitored by Instituto Nicaragüense de Estudios Territoriales (INETER). During periods of extreme degassing the likely-affected population are informed about the specific hazard and, on the basis of recommendations from INETER, protective measures are recommended according to the established protocols of the National System for Disaster Prevention, Mitigation and Attention (SINAPRED). The national park which covers all the Masaya Caldera, or more frequently the viewing platforms near the active Santiago crater, are occasionally closed to the public and tourists during periods of strong degassing [Duffell et al. 2003]. There is no routine monitoring of air quality downwind from the volcano.

The 2016–2019 "Unseen but not unfelt: resilience to persistent volcanic emissions" (UNRESP) Global Challenges Research Fund project investigated resilience to living with persistent volcanic emissions and the environmental pollution hazard they pose, with Masaya as the case study. Here we examine data collected by the UNRESP project using a relatively low-cost gas and particle sensor network of five stations installed in communities near Masaya. This is the first time, to the authors' knowledge, that the performance of low-cost sensors over long-term deployment (six months over February to August 2017) in a volcanic environment is assessed, where the sensors are placed in downwind locations (4–16 km) to determine concentrations of volcanic SO_2 and particulates in distal locations. The robustness and reliability of the network is discussed, in particular the ability of the network to recognise volcanic air pollution episodes (VAPE). We give recommendations for improved set-up and consider other monitoring network instrument options.

2 METHODOLOGY

2.1 AQMesh pods and network set up

AQMesh pods are air quality monitoring systems which cost around £7,000 (~US$9,600) per pod (quote from ACOEM Air Monitors, 2021), relatively low-cost in relation to standard reference-grade instrumentation. Their configuration can be specified by the purchaser allowing a range of possible monitoring options including a variety of gas species, PM, humidity and ambient noise and wind conditions. Gases are measured by electrochemical sensors (B4 series manufactured by Alphasense Ltd). The electrochemical gas sensors and the humidity sensor are mounted into a base plate which allows them to come into contact with the ambient air. Here the gas-measurement focus is on SO_2. PM is measured by an OPC-N2 optical particle counter (manufactured by Alphasense Ltd) which uses a laser beam to detect particles from 0.38 to 17 µm in diameter [Crilley et al. 2018]. Particles are assigned into size fractions of PM_1, $PM_{2.5}$, and PM_{10} using an embedded algorithm developed by AQMesh, and the raw size-resolved data are not available to the user except upon request [AQMesh 2017a]. The AQMesh pods are fitted with a small pump to pass the ambient air through the OPC-N2 which is fitted internally at the top of the instrument. The system is housed in an ABS IP65 box with a mounting bracket for installation. The dimensions are 170 × 220 × 250 mm with an additional 180 mm height if an antenna is fitted [AQMesh 2017b]. The pods weigh between 2 and 2.7 kg depending on sensor and battery configuration. Power is supplied either by mains power at 9–24 V or by an internal lithium metal battery pack at 3.6 V with 273.6 Wh [AQMesh 2017b]. The battery recharging frequency is dependent on the user settings, including the data upload frequency. Here, the pods were used with an internal battery due to unavailability

Table 1: AQMesh pod sensor specifications for Nicaragua installation. Instrument specifications as stated by AQMesh [2017b].

Sensor	Type	Units	Range	Precision	Accuracy	Lower limit
SO_2	Electrochemical	ppbv	0–100,000 ppbv	>0.7	20 ppbv	<5 ppbv
NO	Electrochemical	ppbv	0–20,000 ppbv	>0.9	1 ppbv	<1 ppbv
NO_2	Electrochemical	ppbv	0–20,000 ppbv	>0.85	4 ppbv	<1 ppbv
CO	Electrochemical	ppbv	0–1,000,000 ppbv	>0.8	20 ppbv	<50 ppbv
O_3	Electrochemical	ppbv	0–20,000 ppbv	>0.9	5 ppbv	<1 ppbv
PM	Optical particle counter	$\mu g\ m^{-3}$	0–250,000 $\mu g\ m^{-3}$	>0.85	5 $\mu g\ m^{-3}$	0 $\mu g\ m^{-3}$
Humidity	Solid state	%	0 to 100 %	>0.9	5 % RH	1 % RH

of mains power, and in this study the battery recharge frequency was four weeks. The electrochemical gas sensors and optical particle counter are calibrated during the manufacturing process and have an expected lifespan of two years before replacement is necessary [AQMesh 2017b]. AQMesh pods are manufactured primarily for the monitoring of urban and commercial environments. The measurements are uploaded automatically via mobile network to the AQMesh server which allows data to be downloaded and also to be viewed in tabular and graphical formats. There is an annual fee of £480 (~US$650) for use of the online web server (quote from ACOEM Air Monitors, 2021). The specifications of the sensors used in the AQMesh pods installed in Nicaragua by the UNRESP project are outlined in Table 1.

Five AQMesh pods were installed in settlements to the west of Masaya volcano, downwind of the volcano during prevalent wind conditions. AQMesh pods were installed 1–5 m above the ground. The sites were deemed to have low likelihood of localised pollution sources, with the exception of Rigoberto, which was located on a roof of a home and relatively close to the outlet of domestic cooking fire smoke. The locations of the AQMesh measurement stations and the prevailing plume trajectory are indicated in Figure 2. Based on local knowledge and previous studies [Delmelle et al. 2002; Mather et al. 2003], four of the stations (El Panama, Rigoberto, El Crucero, and Pacaya) are frequently impacted by VAP. San Juan is significantly less likely to be impacted and was therefore used as a background station. El Panama, Rigoberto, and San Juan stations were installed at domestic household sites in low-income rural communities; El Crucero and Pacaya stations were installed in public buildings in more built-up areas. El Panama and Rigoberto are considered near-field stations (~4 km from the crater), and El Crucero and Pacaya are considered far-field stations (~16 km from the crater; Figure 2).

The AQMesh pods were maintained by the UNRESP project and INETER. Technical specifications of the AQMesh pods state that the electrochemical sensors require replacing after 2 years [AQMesh 2017b], however the electrochemical sensors needed replacing several times during the six month experiment period (Table 2). For example, at El Crucero station, issues with the SO_2 sensor and corrosion of the battery connectors required replacement parts to be installed on four occasions within the six months of AQMesh pod deployment, resulting in bad or missing data over 36 % of the measurement time (Table 2). In some instances the internal batteries could not be recharged promptly after four weeks, resulting in periods of missing data due to lack of power. Exposure of the AQMesh pods to a volcanic environment, even in reasonably dilute downwind conditions, likely led to mechanical issues with the pod operating systems [Li et al. 2018]. A high level of fast-acting corrosion impacted the pods at all of the measurement stations, but especially those in closer proximity to the volcanic source point. Corrosion occurred both externally (e.g. to the mounting brackets: Figure 3A, B) and internally (e.g. to the metal parts of the sensors, computer boards and battery charging connectors: Figure 3C, D), resulting in long periods of missing or erroneous data until replacement parts could be installed.

2.2 Sensor Precision and Accuracy

To test the precision of the AQMesh sensors, all pods were placed in proximity together in an urban location (Figure 2) with minimal anthropogenic pollution sources (e.g. away from busy roads), away from volcanic input for an eleven day test period in July 2017. During the co-location test period we simultaneously exposed the PM sensors to episodes of highly elevated particle concentrations from a diesel car exhaust. The pods were placed at the same height and orientation to reduce environmental bias.

To test the accuracy of the SO_2 measurements, two AQMesh pods were co-located with a pulsed fluorescence spectroscopy analyser (Thermo Scientific 43i) for two days in December 2017. The 43i SO_2 analyser is designated by the Environmental Protection Agency (EPA) for measurements in the range of 0–1000 ppbv, with a precision of 1 ppbv and a lower detectable SO_2 limit of 0.5 ppbv [Thermo Scientific 2010; EPA 2016]. The FEM (Forum for Environmental Measurements) designation of instruments, such as this SO_2 analyser,

Table 2: Frequency of AQMesh pods being offline due to sensor failure or corrosion of key components impacting ability to function.

AQMesh number	Installation date	Measurement station	Time in field (days)	Number of occurrences of sensor failure or damage	Number of days with bad or missing data	Percentage of measurement time with bad or missing data
1733150	25/02/17	El Panama	187	5	41	22 %
712150	01/03/17	El Crucero	183	4	66	36 %
789150	27/02/17	Pacaya	184	3	56	30 %
803150	27/02/17	Rigoberto	170	3	19	11 %
735150	28/02/17	San Juan	157	1	8	5 %

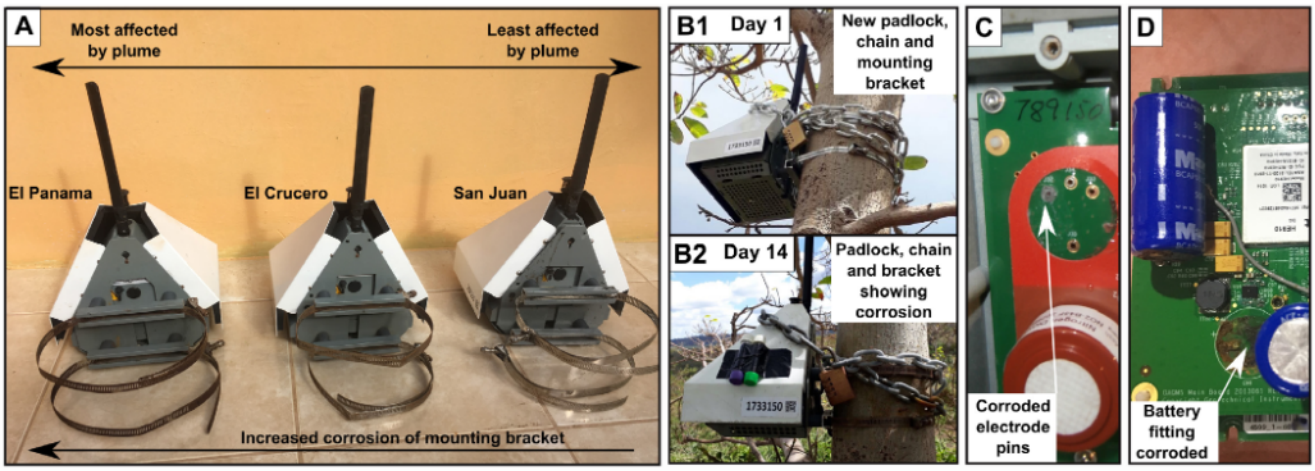

Figure 3: Issues with AQMesh pod corrosion and maintenance. [A] corrosion of metal installation mounting bracket is more advanced in measurement stations more frequently impacted by the volcanic plume; [B] corrosion as a result of the volcanic plume is fast-acting. AQMesh pod 1733150 installed at El Panama with new metal fittings, padlock, and chain [B1] shows obvious signs of corrosion after 14 days [B2]; [C] mounting board for the electrochemical sensors with signs of corrosion on the electrode pins for one of the sensors; [D] an AQMesh internal computer board which controls the sensors showing signs of corrosion with one of the board battery units disconnected.

aims to promote consistency in measurements between different environmental monitoring networks by ensuring that instruments are of reference-grade quality [EPA 2016]. The SO_2 analyser was installed in an air-conditioned building at El Crucero (Figure 2) with an inlet tube feeding air in from outside. AQMesh pods 712150 and 735150 were installed within a few meters of the SO_2 analyser inlet. The SO_2 analyser was calibrated on return to the UK and found to have a baseline drift of 2 ppbv and an underestimation of 18 % [Read 2018]. The SO_2 analyser was verified using a National Physical Laboratory certified Cylinder (Cylinder number: 176433, BOC Ltd) with the blender set-up within the AMOF COZI Laboratory, National Centre for Atmospheric Science (NCAS*).

*https://amof.ac.uk/laboratory/carbon-monoxide-and-ozone-calibration-laboratory-cozi/

2.3 Electrochemical Sensor Cross-Sensitivities

Electrochemical sensors operate by diffusion of the target gas through a porous membrane, following which changes in the chemical potential are measured by a sensing electrode [Austin et al. 2006; Mead et al. 2013]. However, other substances may interfere with the chemical potential of the electrochemical sensor, causing a positive or negative interference to the sensor output, resulting in a biased measurement [Austin et al. 2006; Lewis et al. 2016]. These interfering substances can include a number of compounds, only some of which are reported by the manufacturer. Studies such as Mead et al. [2013] have shown that electrochemical sensors are suitable for monitoring gas levels in low ppbv concentrations, but it must also be recognised that cross-sensitivities of the sensors may have a substantial impact on the sensor output.

The cross-sensitivities of the SO_2-B4 sensor used in

this study can be found in the instrument data sheet*. Of these, cross-sensitivities to NO_2 and O_3 are the most likely to impact the accuracy of the SO_2 measurement [Alphasense 2021]. Changes in temperature and humidity can also impact electrochemical sensor performance [Mead et al. 2013; Lewis et al. 2016]. However, in this study we are not investigating quantitative concentrations of SO_2 but the AQMesh pods' efficiency at determining the simultaneous enhancement of SO_2 and PM and hence the equipment's ability to recognise the presence or absence of volcanic plume, and as such it is sufficient to measure relative changes even when the absolute concentrations of SO_2 are unreliable.

2.4 PM sensor humidity correction factor

The optical particle counter (OPC) used in the AQMesh pods is a small, low-cost sensor making it suitable for deployment in compact instrument systems. Such sensors are becoming widely used in the air quality aerosol-monitoring community as they offer an alternative to more expensive reference-grade instrumentation which often require high power input and surrounding infrastructure [Lewis et al. 2016; Sousan et al. 2016a; b; Kelly et al. 2017]. However, the trade-off of using these low-cost compact OPCs is that they do not currently provide such precise, accurate, or sensitive measurements as their reference-grade counterparts [Sousan et al. 2016a; Crilley et al. 2018; 2020].

Part of the issue lies with the methodology for acquiring the number and size of the particles. Many low-cost OPCs measure the number of particles and the particle diameters by examining the light-scattering as each particle passes through a laser beam. These measurements are then converted to particle mass concentrations by assuming that the particles are spherical and of a uniform density. However, most low-cost OPCs do not dry the sampled air prior to measurement, as this would require additional hardware and power costs. Atmospheric particles are typically hygroscopic in that they absorb moisture from the air, and at high humidities it is often water which is the dominant component of atmospheric particles [Gysel et al. 2007]. The ability of particles to absorb water depends on the particle composition, with the variability of hygroscopicity determined by the inorganic mass fraction, with sulphate in particular being a very hygroscopic particle composition [McFiggans et al. 2005; Gysel et al. 2007; Crilley et al. 2020]. When the sampled air is not dried prior to measurement by OPCs, the particle hygroscopicity can lead to significant bias in the determination of particle size and shape, especially under high humidity conditions [Crilley et al. 2018; Jayaratne et al. 2018; Crilley et al. 2020]. As a consequence of this, the reported particle mass concentrations from OPCs without a heated inlet need to be converted from wet particle mass concentrations to dry particle mass concentrations in order to be more accurate and comparable to reference-grade instruments and measurements made at different humidity levels.

Here we follow the methodology described in Crilley et al. [2018] and Crilley et al. [2020] to apply a correction factor to the reported results for PM_1, $PM_{2.5}$, and PM_{10} from the AQMesh network in Nicaragua. The correction factor (C) is applied in the following manner as described in Equation 1:

$$C = 1 + \left(\frac{\left(\frac{\kappa}{\rho_p}\right)}{-1 + \left(\frac{1}{a_w}\right)} \right) \quad (1)$$

where ρ_p is the density of the dry particles (here we use 1.65 g cm^{-3} which is the ambient particle density assumed by the OPC-N2); a_w is the water activity (RH/100) and the value for κ can be found by a non-linear curve fitting of a humidogram (a_w vs m/m_0 where m and m_0 are the wet and dry (RH=0 %) aerosol mass, respectively). For PM_1 and $PM_{2.5}$ measurements we used a κ value of 0.53 relating to ammonium sulphate [Petters and Kreidenweis 2007] and for PM_{10} measurements we use a κ value of 0.33 relating to dust particles as these have a lower hygroscopicity and would normally be found in the PM_{10} size fraction [Pringle et al. 2010]. For the correction factor calculations we use the relative humidity as measured by the humidity sensor installed in the base plate of the AQMesh pods.

The raw particle mass concentrations reported by the AQMesh pods can then be corrected according to Equation 2:

$$PM_{Corr} = \frac{PM_{Raw}}{C} \quad (2)$$

The manufacturer states that the OPC-N2 instruments are factory calibrated prior to sale. The application of the correction factor as described above should remove the impact of high humidity conditions from the measurements [Crilley et al. 2018; 2020].

2.5 Detecting volcanic air pollution episodes

By definition, VAP elevates concentrations of SO_2 and PM at ground level for a period of time. However, the SO_2 sensors periodically recorded seemingly unrealistic peaks and troughs in concentration (Figure 8). Therefore, we attempted to evaluate how reliable the AQMesh pods are in identifying VAPE by using different data analyses approaches and independent sources of data. We analysed the AQMesh data for correlations between SO_2 and PM and for variability in PM concentrations and size fractions. Forecast meteorological data (ECMWF) and high-resolution satellite images of the volcanic plume were used as independent proxies for the likely presence of VAPE.

*https://www.alphasense.com/WEB1213/wp-content/uploads/2019/09/SO2-B4.pdf

2.5.1 *Concurrent SO_2 and PM*

We expect a strong correlation between SO_2 and PM during VAPE as both species are abundant in volcanic plumes. SO_2 has no strong non-volcanic local sources (some amounts are emitted from cooking fires and fuel combustion) and would therefore only become elevated at ground level during VAPE. PM is released in high concentrations both from volcanic and non-volcanic origins (likely local sources include cooking fires, traffic, household waste burning and agricultural fires) and would become elevated during both types of pollution events. SO_2 alone, or the simultaneous presence of both SO_2 and PM, will distinguish episodes of volcanic pollution from non-volcanic pollution.

The data obtained from the AQMesh instruments were processed into hourly averages. Periods of erroneous or missing data (Table 2) were not included in the analysis. The remaining data were analysed using `RatioCalc 3.2` software following Tamburello [2015]. `RatioCalc` software was used to determine periods of time when there were strong correlations (r^2 greater than 0.5) between SO_2 and the humidity-corrected measurements of PM_1, $PM_{2.5}$, and PM_{10} (henceforth termed simultaneous enhancement of SO_2 and PM) indicating VAPE. A minimum threshold of four consecutive days of good correlation was set to ensure that the concurrent SO_2 and PM signal was real and not a result of instrumental error or drift. Data were excluded from further analysis when SO_2 had a correlation to the relative humidity greater than an r^2 value of 0.25, as a dependence on humidity indicates the SO_2 response is not representative of the actual atmospheric SO_2 concentrations but an instrumental artefact. Correlation periods were only included where SO_2 concentration peaks reached at least 20 ppbv, as concentrations lower than this are beneath the unambiguous detection limit of the electrochemical SO_2 sensor. At Rigoberto station, the AQMesh pod recorded some instances where SO_2 concentrations peaked at 300 ppbv for short (< 3 hour) durations. Such peaks in SO_2 were not found elsewhere during the analysis and have been interpreted to be anthropogenic pollution, most likely from the local cooking fires. These cooking fire–related detections were removed from the analysis.

2.5.2 *PM concentration and size fractions*

We analysed the concentration and change in size fractions of PM_1, $PM_{2.5}$, and PM_{10} from each of the measurement stations. Using the VAPE identification from ECMWF and satellite imagery (respective methods in Section 2.5.3 and Section 2.5.4), the PM data were divided into categories of VAPE-likely and VAPE-unlikely conditions and analysed to investigate any significant differences in the number and range of PM under the different conditions. A two-sample t-test, used to test whether the means of two datasets are equal, was applied to determine the significance level of any differences between the VAPE-likely and VAPE-unlikely conditions for each of the size fraction categories. Using the VAPE-unlikely dataset, a monthly average background concentration was calculated for each PM size category at each measurement station. The VAPE-likely and VAPE-unlikely datasets were then compared to the monthly background average to determine significant outliers indicating PM pollution events.

2.5.3 *ECMWF Forecast Data*

We used meteorological data to determine the likely volcanic plume transport direction, as an indication for how likely VAPEs were during a particular period. Observations from meteorological stations could not be obtained within the scope of this project. Instead we used forecast meteorological data from the European Centre for Medium-Range Weather Forecasts (ECMWF) to determine when volcanic plume was likely to have been present at the measurement stations. ECMWF uses ensemble forecasting to predict the evolution of atmospheric conditions through time [Molteni et al. 1996; Buizza et al. 2005]. Forecast data were extracted from the ECMWF model at 12.0000 N 273.8750 E, which is the closest grid point to Masaya volcano, located approximately 1 km to the north and 3 km to the west from the active volcanic vent. The ECMWF forecast resolution was 0.125 degrees (~12 km at the equator).

ECWMF forecasts were obtained for the period 27th February to 28th August 2017. Data were retrieved in a three-hour cycle, with each output producing forecast results at twenty-five pressure levels through the atmosphere, from 1000 hPa (average geopotential height of 104 m asl) to 1 hPa (average geopotential height of 46,197 m asl). Model estimates of temperature (K), wind direction (° from north), wind speed ($m\,s^{-1}$), geopotential height (m), vertical velocity ($m\,s^{-1}$) and humidity (% RH) were extracted for each pressure level. The wind speed and direction were examined graphically in wind roses to determine changes in the wind direction through a vertical profile of the atmosphere from near ground-level to 3000 m asl. The predominant wind direction was found to be from an East or East-North-East direction for the lower 3000 m of the atmospheric column during the period of interest.

The wind direction at each pressure level, derived from the ECMWF forecasts, was compared to the wind direction derived visually from visible plume extension seen in satellite imagery (Section 2.5.4) to determine best correlation and likely height of the plume. The time of satellite imagery acquisition was obtained from the image metadata, and the comparison to ECMWF forecasts was calculated at the closest model output time to reduce discrepancies from changes in wind direction before and after satellite imagery acquisition.

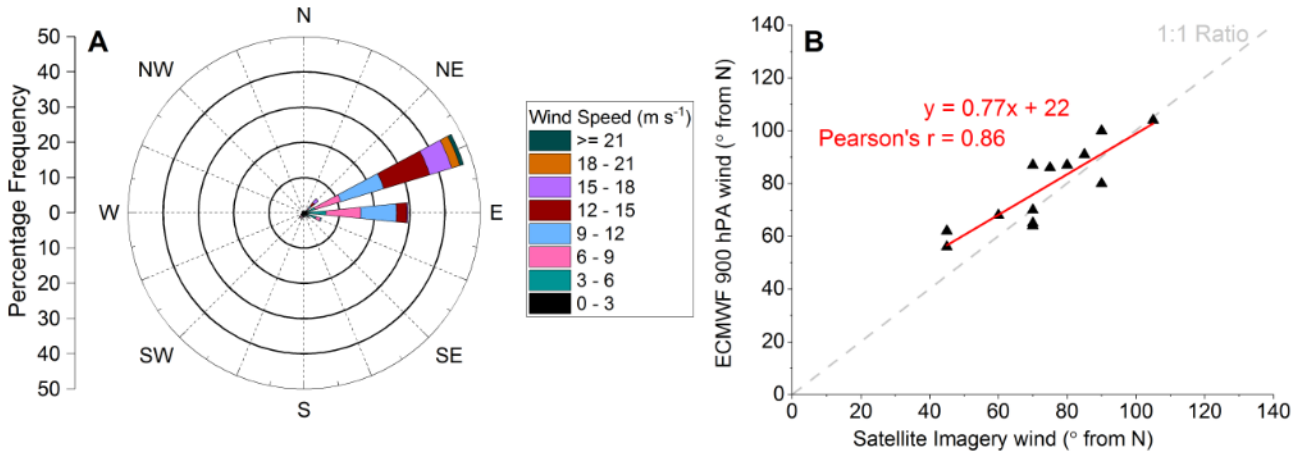

Figure 4: Forecast meteorological data for Masaya volcano. [A] Wind rose for the period February to August 2017 at 900 hPa, with an average geopotential height of 948 m ± 113 m. Wind direction is predominantly from the ENE and E. Data are derived from ECMWF forecast and are displayed as the direction the wind is blowing from. [B] Comparison between the ECMWF 900 hPA wind direction data and the wind directions derived from the satellite imagery over Masaya volcano.

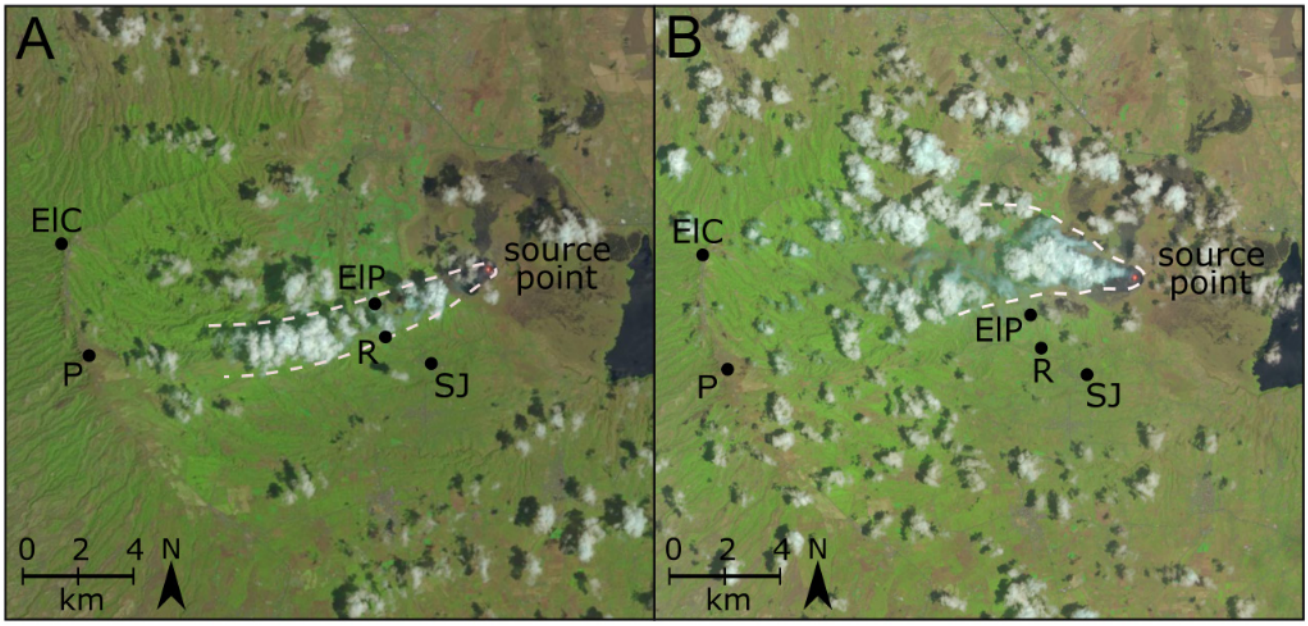

Figure 5: Satellite imagery obtained from the USGS Landlook viewer, annotated with plume trajectories indicated by white dashed lines. The source point (Masaya volcano's Santiago crater) is visible with the lava lake. AQMesh measurement stations are indicated with black circles and labelled as follows: EIC - El Crucero; P - Pacaya; EIP - El Panama; R - Rigoberto; SJ - San Juan. Plume is visible by semi-linear feature of white condensing clouds initiating from the source point, often interspersed with blue-tinged haze which is likely due to the particulate component. [A] 13th March 2017 where the plume moves initially towards the south-west before the trajectory alters towards the west. Plume width is approximately 1.5 km. [B] 30th March 2017 where the plume moves west with a wide lateral spread of approximately 3 km within the first 4 km from the source point.

The ECMWF forecast at 900 hPa (948 m ± 112 m asl) had the highest correlation with plume extension orientation seen in satellite imagery during the thirteen days of overlapping data, with a Pearson's r value of 0.86 (Figure 4). As a result we interpret that the plume is most commonly being dispersed away from Masaya volcano at a geopotential height of 948 m asl. This is consistent with the volcano summit height (635 m asl) plus some thermal plume rise above the crater. However, we recognise that this interpreted plume height may have some bias resulting from only using visible plume extension from satellite imagery on days with

clear skies if we consider that overcast days may have a different air pressure causing the plume to travel at a different height in the atmosphere. The ECMWF forecast at 900 hPa were used throughout the study to determine which AQMesh station was likely exposed to volcanic plume throughout the period of interest. We recognise that using ECMWF forecast data at an average height in the atmosphere of 948 m asl to interpret the dispersion direction of Masaya's volcanic plume may introduce errors in the prediction of which AQMesh station was exposed to volcanic pollutants as there is no guarantee that the plume will "ground" at the AQMesh station to allow ground-based measurement of the pollutants. ECMWF forecast data were used in 24-hour averages to give a good representation of the overall meteorological conditions. The likely presence of plume at each AQMesh measurement station was evaluated and compared to the AQMesh measurements to quantify the effectiveness of the AQMesh pods at recognising the presence of volcanic plume.

2.5.4 *Satellite Imagery*

Visual satellite imagery of the volcanic plume from Masaya was used as another indication for a greater likelihood of a VAPE. The USGS Landlook Viewer* displays high-resolution satellite images from Sentinel 2, Landsat 7, and Landsat 8. The satellite imagery obtained was non-continuous over 2017. Twenty-seven satellite images were obtained of the region around Masaya volcano between 5th March and 28th August 2017. Of these, twelve could not be effectively examined to determine plume direction due to the extent of opaque cloud cover, and two occurred during periods of unavailable ECMWF data. The remaining thirteen satellite images were compared to the ECMWF forecast wind directions. Visual inspection of the plume trajectory was also used to determine which AQMesh station was likely exposed to volcanic plume on a given day.

Visual analysis of the satellite imagery suggested sources of potential errors in the identification of likely plume presence at an AQMesh station using the ECMWF forecasts. Some satellite imagery indicated non-linear movement of Masaya's volcanic plume. A non-linear plume trajectory (Figure 5A) may result in bias in the assignment of which AQMesh station was likely exposed to volcanic plume, as the wind direction does not remain constant following plume dispersal away from the source point. As there is limited availability of satellite imagery for use in comparison to the ECMWF data, it is not possible to determine the frequency of occurrences of non-linear plume trajectory. Another potential source of error is the width of the plume. Figure 5A and 5B indicate the variability in lateral plume width (by a factor of ~2), which is not determinable from the ECMWF forecast wind direction and may cause errors when characterising stations as being likely exposed to VAP on a specific day. Satellite imagery also suffers from the same "grounding" uncertainty where it is not certain that a visible plume is reaching the Earth's surface.

*https://landlook.usgs.gov/

3 RESULTS

3.1 Precision of AQMesh Pods PM Measurements

During the co-location testing period (section 2.2) the SO_2 concentrations were low and within the noise limit for the electrochemical sensors. As such, only the PM measurements from this co-location period were considered, the results of which for PM_1 and $PM_{2.5}$ are shown in Figure 6. During the testing period, the PM_1 concentrations were less than 15 $\mu g\,m^{-3}$ and the $PM_{2.5}$ were less than 30 $\mu g\,m^{-3}$.

The PM measurements of each of the five AQMesh pods were analysed and assessed for correlation during the co-location period. For PM_1 measurements, Pearson's r values were high between instruments, with 30 % of the r values above 0.9 and 60 % above 0.8. However there was significant variability in the magnitude of PM recorded, with AQMesh pods 712150 and 789150 consistently measuring higher values than pods 803150, 1733150, and 703150. For $PM_{2.5}$ measurements, similar Pearson's r values were found, with 20 % above 0.9 and 70 % above 0.8. Measurement variability was reduced in $PM_{2.5}$ measurements, though pod 712150 consistently reported lower values with respect to the other instruments (Figure 6).

The co-location indicated that there was some significant variability between the OPC-N2 instruments within the AQMesh pods at low concentrations. However, despite the variability in absolute measurements, all the instruments recorded high concentrations simultaneously, suggesting that the AQMesh pods are suitable for monitoring increases in PM above background concentrations, even if there is variability in the absolute concentration of PM recorded.

3.2 Accuracy of AQMesh Pod SO_2 Measurements

During the testing period of AQMesh and the pulsed fluorescence spectroscopy SO_2 analyser (Section 2.2), both co-located AQMesh pods underestimated the concentrations measured by the SO_2 analyser by up to 75 % (Figure 7). The correlation between the electrochemical sensors and the SO_2 analyser was very good, with Pearson's r values of 0.92 and 0.93 respectively across both AQMesh pods. The two AQMesh pods correlated very well with each other, with a Pearson's r value of 0.98 and 5 % variance in the measurement trend (Figure 7C). The Alphasense B4 sensors may not be suitable for reporting absolute values of SO_2 at low concentrations (see discussion below), but are reliable for detecting when SO_2 in the atmosphere is increased to

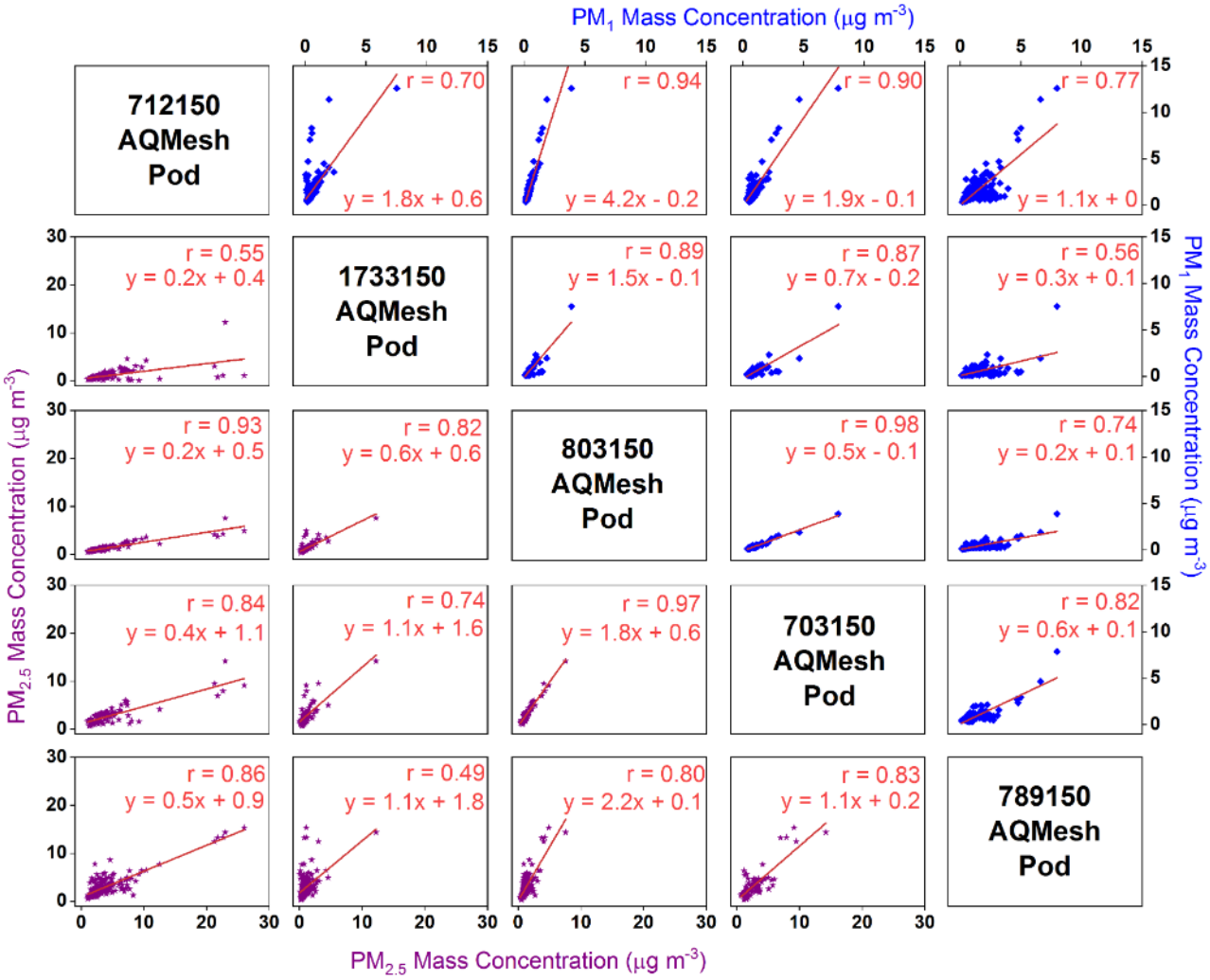

Figure 6: Scatter plot matrix of PM_1 and $PM_{2.5}$ results from co-location of AQMesh pods for eleven days in July 2017, all data are in hourly averages. PM_1 results are displayed in the ten plots in the upper triangle with data plotted in blue. $PM_{2.5}$ results are displayed in the ten plots in the lower triangle with data plotted in purple. All data presented have been processed with the correction factor outlined in Section 2.4.

above background concentrations. We therefore suggest that they are suitable for a low-cost sensor network where the instruments are used to determine the presence or absence of volcanic plume and where identifying changes is the greatest priority.

Although AQMesh indicates that the SO_2 sensors were calibrated in the factory prior to sale, it is likely that each electrochemical sensor will have a slightly different level of accuracy and measurement precision with the potential for some baseline drift [Alphasense 2021]. The impact of the corrosive volcanic environment was the likely cause of the SO_2 electrochemical sensors frequently failing and requiring replacement. This means that there will be temporal inconsistencies as sensors are replaced, adding an additional source of uncertainty to the data. One of the symptoms of the SO_2 sensor failures was extreme peaks and troughs in the recorded SO_2 (Figure 8). These peaks and troughs were not recorded at the background measurement station at San Juan, or at the Rigoberto measurement station which was located closer to the edge of the prevailing plume dispersion region (Figure 8A, B). The near-field site at El Panama and the far-field sites at El Crucero and Pacaya recorded extreme peaks and troughs in SO_2 (Figure 8C–E), likely due to SO_2-induced corrosion. SO_2 measurements at some AQMesh stations recorded a diurnal signal which is likely due to the humidity and/or temperature impacting the sensor baseline (Figure 8F, I). These diurnal signals are difficult to remove as each SO_2 sensor can have sensor-specific responses and several sensors had to be replaced during the six-month experiment period. Due to the frequent SO_2 sensor failure and extreme erroneous measurements, the SO_2 data is here concluded to be unreliable as a stand-alone measurement, at least for long-term deployment with minimal maintenance commitment. This further motivates our methodology choice to use simultaneous enhancement of SO_2 and

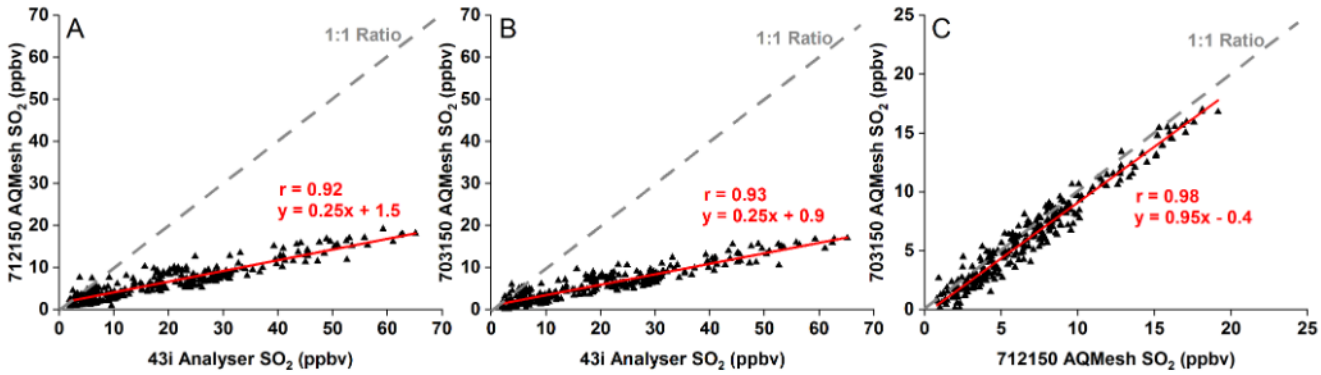

Figure 7: Co-location of 43i SO_2 analyser and two AQMesh pods at El Crucero measurement station. Comparisons of SO_2 measurements between [A] 43i analyser and the SO_2 electrochemical sensor in the 712150 AQMesh pod; [B] 43i analyser and the SO_2 electrochemical sensor in the 703150 AQMesh pod; [C] SO_2 electrochemical sensor in the 712150 AQMesh pod and the SO_2 electrochemical sensor in the 703150 AQMesh pod. Comparisons and data presented here are the peaks in data, near-baseline measurements were removed as they were within the baseline noise fluctuations of the AQMesh sensors. Measurements from the 43i analyser have been corrected to remove baseline drift and to account for 18 % underestimation as indicated by post-fieldtrip calibration.

PM (i.e. correlation with $r^2 > 0.5$, see Section 2.5.1) as an indicator of the presence of volcanic plume (Figure 9).

3.3 Efficiency of AQMesh pods at recognising volcanic plume

3.3.1 *Simultaneous enhancement of SO_2 and PM indicates VAP*

Wind directions from the ECMWF 900 hPa forecast and the satellite imagery were analysed to determine when VAPE was likely to be present at an AQMesh measurement station. The VAPE-likely days were cross-referenced with the AQMesh data periods of simultaneously elevated SO_2 and PM to determine the ability of the instruments to detect VAPE. This approach will miss identification of VAPE by the instruments when the sensors recorded simultaneously elevated SO_2 and PM for less time than our defined minimum threshold of four consecutive days. The results are presented in Figure 10.

A control analysis was implemented to identify agreement-positives (where ECMWF or satellite imagery indicated VAPE-likely at the same time as the AQMesh instruments also detected a simultaneous enhancement of SO_2 and PM) and disagreement-positives (where ECMWF or satellite imagery indicated VAPE-unlikely but the AQMesh instruments reported a simultaneous enhancement of SO_2 and PM). It should be noted that the determination of VAPE from the ECMWF data and satellite imagery may have substantial bias (see Section 2.5.3 and Section 2.5.4). The meteorological data is a forecast rather than an observation, and therefore there may be instances of the plume being present at a measurement station without the forecast successfully predicting its presence. The forecast may also not successfully predict whether the plume is at ground level. The potential bias of the satellite imagery is caused by the fact that the images are a snapshot in time and do not capture conditions where the plume direction is dynamic. The results of the control analysis are presented in Figure 11.

At the background San Juan station (Figure 2), the AQMesh pod detected no simultaneous enhancement of elevated SO_2 and PM. ECMWF data and satellite imagery indicated no intervals of VAPE-likely, in agreement with the AQMesh.

At the near-field sites (Rigoberto and El Panama), the AQMesh pods detected the presence of the plume in reasonably good agreement with the ECMWF and satellite imagery given the potential sources of bias detailed above. At El Panama the AQMesh pod detected the plume with elevated SO_2 and $PM_{2.5}$ for 65 % of the time that ECMWF indicated VAPE-likely, and 42 % of the time that satellite imagery indicated VAPE-likely (Figure 10). The AQMesh at Rigoberto identified the presence of the plume with elevated levels of SO_2 and $PM_{2.5}$ for 42 % of the time that ECMWF indicated VAPE-likely and 30 % of the time that satellite imagery indicated VAPE-likely (Figure 10). The results were very similar for SO_2/PM_1 and $SO_2/PM_{2.5}$ correlations. For SO_2/PM_{10} correlation the plume was less often identified at El Panama and never at Rigoberto. Null-hypothesis tests were then performed on the data sets with VAPE-likely or VAPE-unlikely defined according to combined ECMWF and satellite imagery methods (Figure 11). The null-hypothesis test at the near-field sites indicated a much higher level of agreement-positive than disagreement-positive results

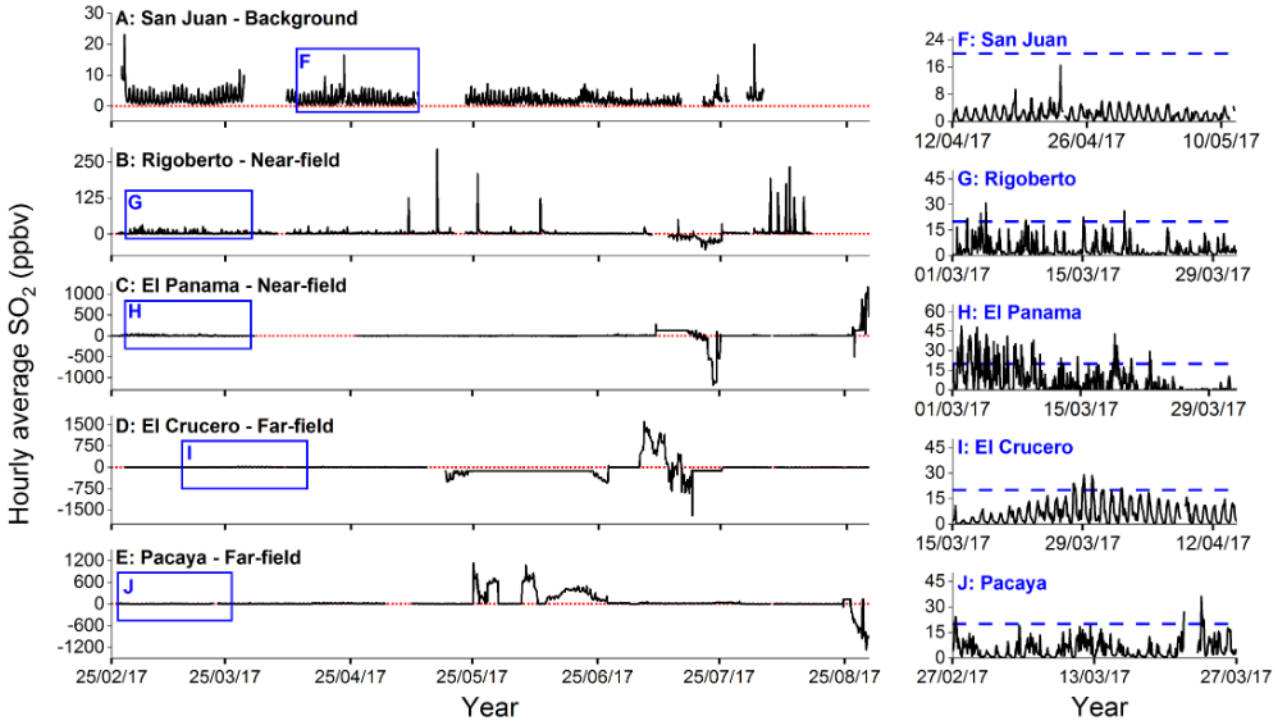

Figure 8: Electrochemical SO_2 measurements from the five AQMesh stations. [A–E]: timeseries of hourly-average electrochemical SO_2 measurements over the six-month experiment period. Periods of missing data result from lack of power due to corroded battery connectors or batteries remaining uncharged after four weeks. Extreme SO_2 peaks and troughs result from failure of the SO_2 electrochemical sensors. Red dashed line indicates 0 ppbv line. Blue outlines indicate time-periods for F–J. [F–J]: 1-month excerpts from the SO_2 timeseries at each AQMesh station, indicating periods of data with no extreme peaks and troughs. Blue dashed line indicates 20 ppbv, the lower limit used for identifying periods of simultaneously enhanced SO_2 to PM.

for both AQMesh stations. At El Panama station the AQMesh pod recorded agreement-positive identifications of VAPE 59 % of the time for SO_2 and PM_1, 61 % of the time for SO_2 and $PM_{2.5}$, and 46 % of the time for SO_2 and PM_{10} (Figure 11). There were significantly lower numbers of disagreement-positive plume identifications at El Panama, at 18 % for PM_1 and PM_{10} and 23 % for $PM_{2.5}$ (Figure 11). Rigoberto AQMesh pod likewise had a higher percentage of agreement-positive instances than disagreement-positives for simultaneously elevated SO_2 and PM_1 (41 % agreement-positive and 22 % disagreement-positive) and $PM_{2.5}$ (41 % agreement-positive and 15 % disagreement-positive), with no occasions of correlations in SO_2 and PM_{10} at $r^2 > 0.5$. However, the absolute number of disagreement-positive identifications was higher at Rigoberto for SO_2 to PM_1, with 16 agreement-positive events and 21 disagreement-positive events. Rigoberto station was located closer to the edge of the prevailing plume dispersion region (Figure 2) and also relatively close to domestic cooking fires and the occurrences of disagreement-positives at this measurement site may be due to pollution events not related to Masaya volcano.

The far-field sites situated on the Las Sierras highlands (El Crucero and Pacaya) were not able to effectively recognise the presence of volcanic plume via means of simultaneously elevated SO_2 and PM. The El Crucero AQMesh pod recognised a volcanic signature 5 % of the time that ECMWF indicated VAPE-likely at the station, and 0 % of the time that satellite imagery indicated VAPE-likely (Figure 10). The AQMesh at Pacaya never detected VAPE as defined by simultaneous enhancement of SO_2 and PM. Likewise the null-hypothesis test at the far-field sites indicated that the far-field AQMesh pods were not able to effectively recognise the presence or absence of the volcanic plume. El Crucero AQMesh station had an equal percentage of agreement-positive and disagreement-positive events for SO_2 to PM_1, and no periods of simultaneously elevated SO_2 and $PM_{2.5}$ or PM_{10}. The likely reasons for this are discussed in Section *4.1.2*.

The agreement in VAPE identification was higher between AQMesh and ECMWF than between AQMesh and satellite imagery for El Panama, Rigoberto and El Crucero stations (Figure 10). This is potentially due to satellite images providing only a snapshot of the meteorological conditions, whereas the ECMWF data were analysed as daily averages to provide an overview of conditions and reducing the impact of outlying wind directions.

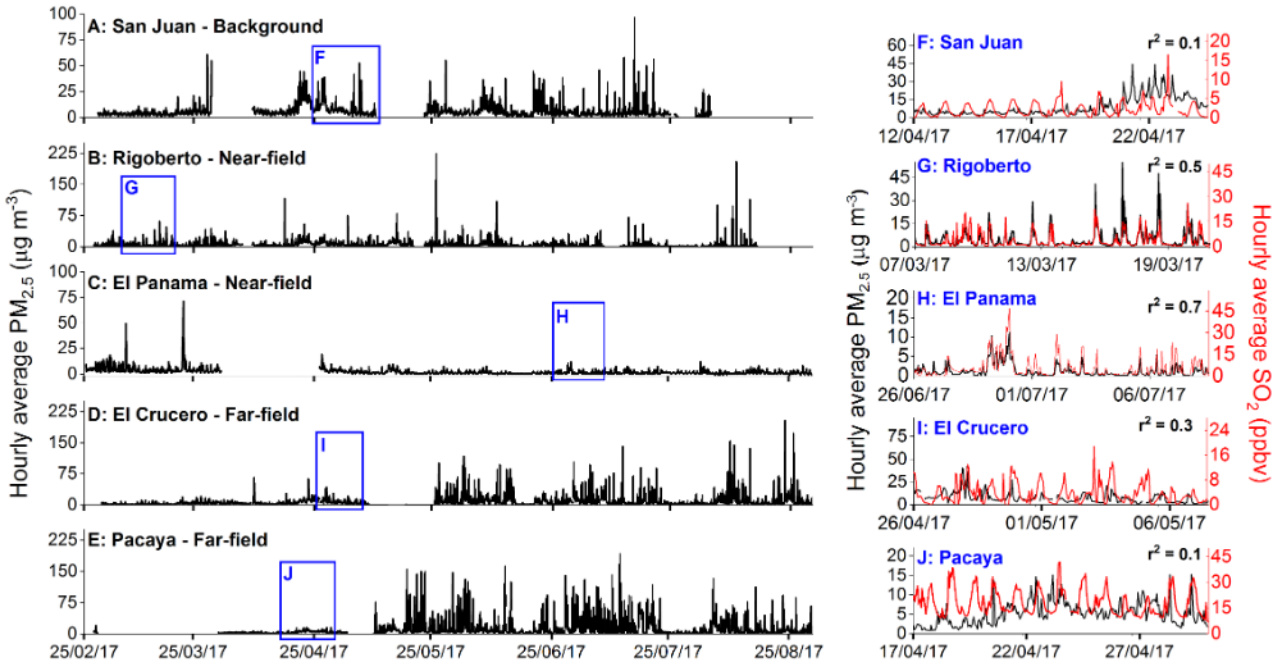

Figure 9: $PM_{2.5}$ measurements from the five AQMesh stations. [A–E]: timeseries of hourly-average $PM_{2.5}$ measurements over the six-month experiment period, with all results corrected for humidity using the method outlined in Section 2.4. Periods of missing data result from lack of power due to corroded battery connectors or batteries remaining uncharged after four weeks. Blue outlines indicate time-periods for F–J. [F–J]: 14-day excerpts from the $PM_{2.5}$ timeseries at each AQMesh station. SO_2 measurements for the same time-period indicated by the red dataline, with corresponding scale on the right-hand y-axis. Correlation between $PM_{2.5}$ and SO_2 for the excerpt period is indicated in the top-right corner of each plot. Time-periods for the 14-day excerpts were chosen where $PM_{2.5}$ and SO_2 data were both available (with no extreme SO_2 peaks or troughs), and where there were simultaneous elevations of SO_2 and PM, if available.

3.3.2 *Enhancement in fine PM associated with the presence of volcanic plume*

PM data were analysed to determine whether there were significant differences in the mass concentrations of different size fractions (PM_1, $PM_{2.5}$, and PM_{10}) under VAPE-likely and VAPE-unlikely conditions. A two-sample t-test indicated significant differences in the mean PM under VAPE-likely and VAPE-unlikely conditions at El Crucero and El Panama with all probabilities well below the significance level of 0.05. The two-sample t-test at Pacaya also showed significant difference between VAPE-likely and VAPE-unlikely conditions, although with probabilities closer to the significance level of 0.05. Rigoberto data proved to have an insignificant difference between the VAPE-likely and VAPE-unlikely conditions for all size fractions. A two-sample t-test could not be calculated for San Juan AQMesh station as ECMWF and satellite imagery did not indicate any periods where the plume was likely to have been present there, consistent with it being a background site. At El Panama and El Crucero, the two-sample t-test indicated a larger significance in the difference between VAPE-likely and VAPE-unlikely conditions for PM_1 than for the larger size fractions, while at Pacaya the highest significance was for $PM_{2.5}$ followed by PM_1. This indicates that the majority of the volcanic PM are very fine (typically <1 µm diameter), which follows the findings of previous studies where volcanic PM are often found to be in the smallest size fraction [Martin et al. 2011; Ilyinskaya et al. 2017; 2021; Mason et al. 2021].

Peaks in PM concentrations for each size fraction do not appear to be linked to the presence or absence of the plume, with equally high maximum hourly concentrations recorded under both VAPE-likely and VAPE-unlikely conditions (Figure 12). However, at El Panama and El Crucero, the average PM concentration across the six-month measurement period for all size fractions is higher during VAPE-likely conditions than VAPE-unlikely conditions (Figure 12), as was shown by the t-tests above. This is in agreement with observations of a PM-rich volcanic plume in Iceland [Ilyinskaya et al. 2017]. From this we infer that at these stations there is a background level of PM that persists under both VAPE-unlikely and VAPE-likely conditions, whilst in VAPE-likely conditions there is an additional contribution from volcanically-sourced PM.

We calculated the frequency of episodes when PM size-dependent concentrations are above-background

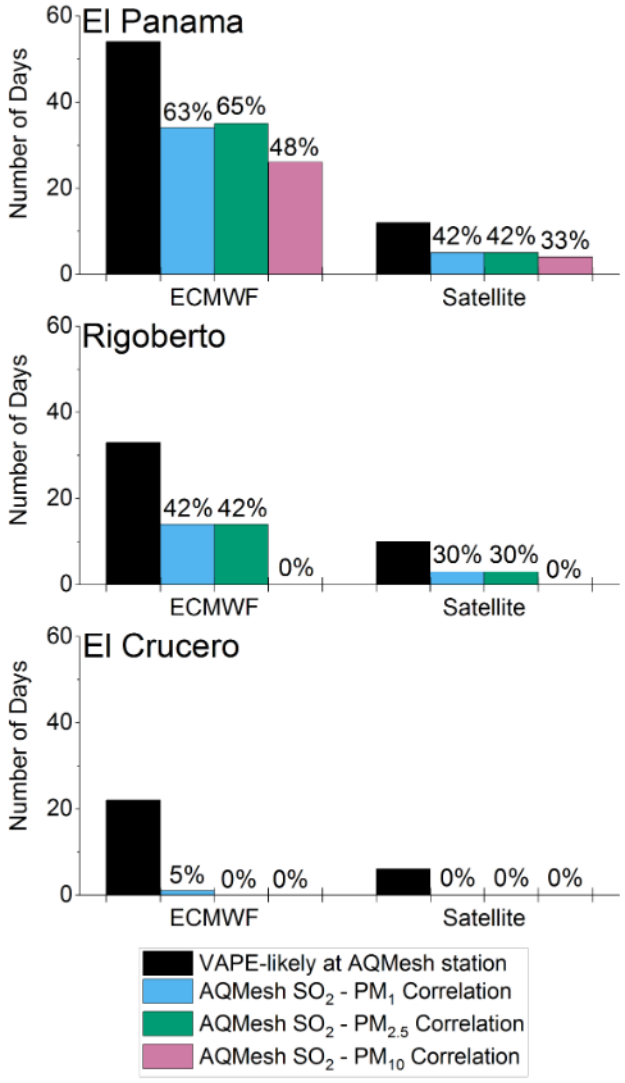

Figure 10: Efficiency of AQMesh pods at recognising VAPE derived from satellite and ECMWF data at three measurement stations. The frequency of VAPE-likely periods at the measurement station is indicated by the black bar, and frequency of simultaneous enhancement of SO_2 and PM AQMesh measurements are indicated by the blue, green and pink bars. Only periods where the AQMesh instrument was functional are considered here. Results are split into VAPE-likely periods derived from ECMWF forecasts and from satellite imagery. Percentages noted on each coloured bar indicate the proportion of how often that the AQMesh pods recognised VAPE derived from the relevant meteorological data. San Juan and Pacaya AQMesh stations are not displayed as no simultaneous enhancement of SO_2 and PM were found at these stations.

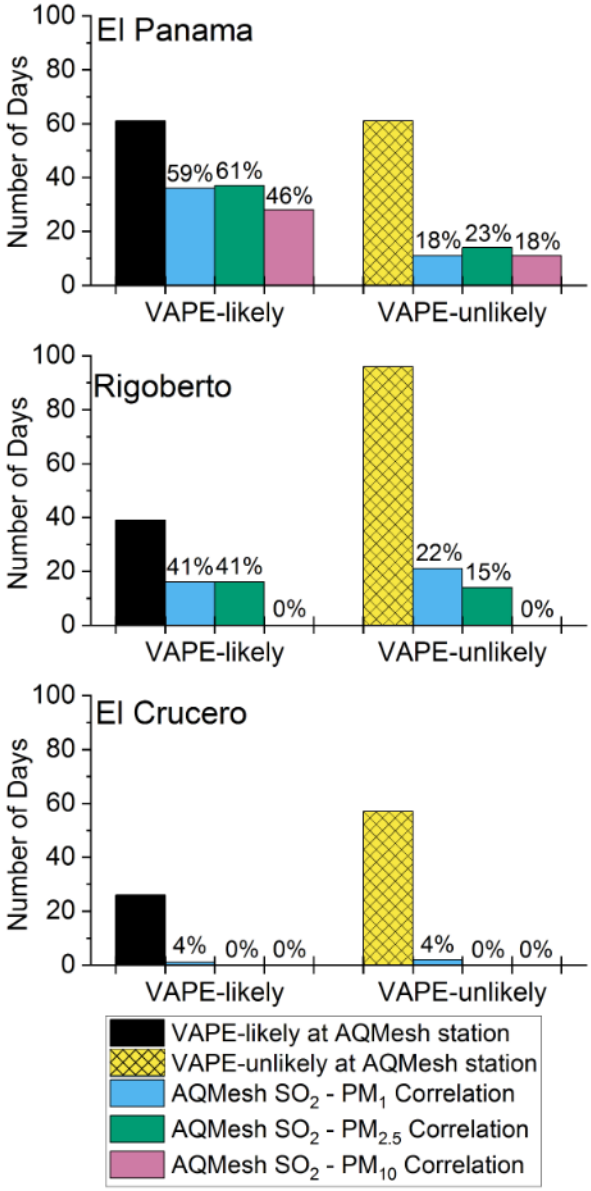

Figure 11: Efficiency of AQMesh pods at recognising VAPE at three measurement stations. Black bars indicate frequency of VAPE-likely conditions at the measurement station, as derived from both ECMWF and satellite data, during periods when the AQMesh pod was fully-functional. Yellow hatched bars indicate frequency of VAPE-unlikely conditions at the measurement station, as derived from both ECMWF and satellite data, during periods when the AQMesh pod was fully-functional. Percentages noted on each coloured bar under VAPE-likely conditions indicate the proportion of how often that the AQMesh pods recognised VAPE by means of simultaneous enhancement of SO_2 and PM. Percentages noted on each coloured bar under VAPE-unlikely conditions indicate the proportion of how often that the AQMesh pods gave a disagreement-positive result and falsely indicated VAPE. San Juan and Pacaya AQMesh stations are not displayed as no simultaneous enhancement of SO_2 and PM were found at these stations.

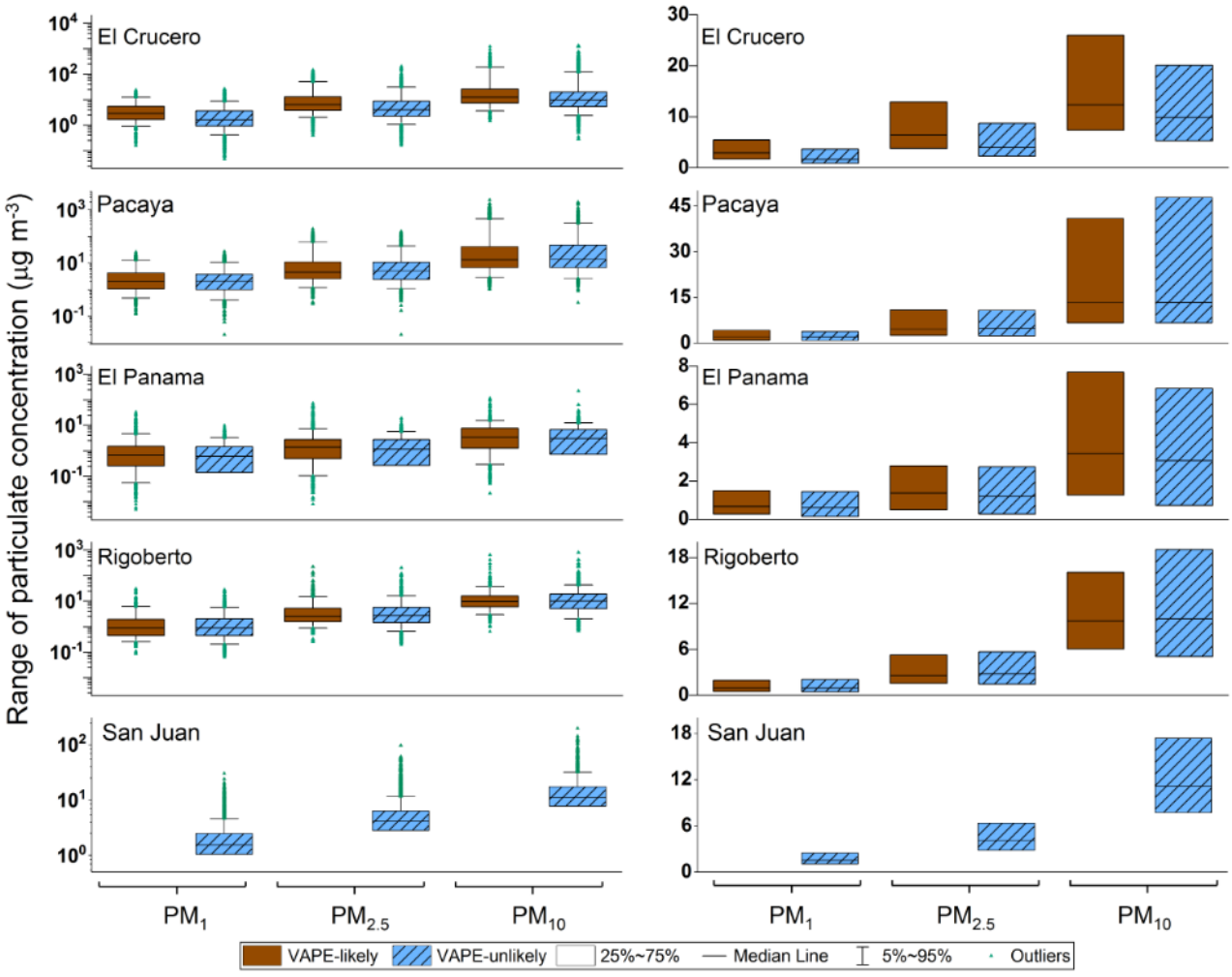

Figure 12: Range of PM concentrations at El Crucero, Pacaya, El Panama, Rigoberto, and San Juan measurement stations under VAPE-likely (brown box-plots) and VAPE-unlikely (blue box-plots) conditions. Note the logarithmic y-axis scale on the left-hand graphs and linear y-axis scale on the right-hand graphs. VAPE-likely or VAPE-unlikely conditions are as identified by ECWMF forecasts and satellite imagery. Data plotted are hourly averages across the entire measurement period.

(Table 3). We identified events where the average daily concentration exceeded one standard deviation above the long-term background average, indicating a PM pollution event (hereafter termed as such). At El Panama there was a much higher frequency of PM pollution events during VAPE-likely periods (41 % for PM_1, 40 % for $PM_{2.5}$, and 44 % for PM_{10}) than during VAPE-unlikely periods (17 % for PM_1, and 21 % for both $PM_{2.5}$, and PM_{10}) (Table 3). The El Crucero measurement station had a higher frequency of PM pollution events during VAPE-likely conditions (48 % for both PM_1 and $PM_{2.5}$ and 25 % for PM_{10}) than during VAPE-unlikely conditions (8.6 % for PM_1, 5.5 % for $PM_{2.5}$, and 13 % for PM_{10}). Enhanced frequency of PM pollution events during VAPE-likely periods is also seen at the Pacaya and Rigoberto stations but it is much smaller than at the other stations (Table 3). At the background San Juan station, the frequency of PM pollution events was comparable to VAPE-unlikely periods at the other stations (Table 3). This supports the interpretation that AQMesh pods are reliably identifying PM pollution events of volcanic vs non-volcanic origin.

4 Discussion

4.1 Detection of VAP from Masaya volcano by AQMesh network

4.1.1 *Near-source locations impacted by the plume*

The AQMesh pods at both El Panama and Rigoberto were reasonably effective at recognising the presence of volcanic plume as defined by simultaneous enhancement of SO_2 and PM during periods when meteorological data suggested the plume was likely at the

Table 3: PM pollution events defined as a period of 24-hours exceeding 1 standard deviation (SD) above the monthly background 24-hour PM average. VAPE-likely and VAPE-unlikely conditions are determined from ECMWF data and satellite imagery, and the monthly background average concentration is calculated from the VAPE-unlikely period data. The percentage of time exceeding the background average is calculated from the total time under VAPE-likely or VAPE-unlikely conditions.

Station location	PM size group	Events exceeding 1∼SD above background average		Percentage time exceeding 1∼SD above background average	
		VAPE-likely Conditions	VAPE-unlikely Conditions	VAPE-likely Conditions	VAPE-unlikely Conditions
El Crucero	PM_1	19	11	48 %	8.6 %
	$PM_{2.5}$	19	7	48 %	5.5 %
	PM_{10}	10	16	25 %	13 %
Pacaya	PM_1	16	13	22%	18 %
	$PM_{2.5}$	18	15	25 %	20 %
	PM_{10}	13	14	18 %	19 %
El Panama	PM_1	33	14	41 %	17 %
	$PM_{2.5}$	32	18	40 %	21 %
	PM_{10}	36	18	44 %	21 %
Rigoberto	PM_1	9	20	21%	16%
	$PM_{2.5}$	6	20	14 %	16 %
	PM_{10}	6	18	14 %	15 %
San Juan	PM_1	0	19	0 %	14 %
	$PM_{2.5}$	0	20	0 %	15 %
	PM_{10}	0	19	0 %	14 %

measurement station. Both stations also had a number of plume identifications during intervals when the meteorological data suggested VAPE-unlikely conditions, though the percentage of disagreement-positives was smaller than the percentage of agreement-positives (Figure 11). These findings support that simultaneous enhancement of SO_2 and PM measured by the AQMesh in near-field measurement stations around Masaya volcano are a suitable indicator for recognising the presence of the volcanic plume.

The PM distribution analysis indicated that the El Panama AQMesh pod recorded significantly higher frequencies of PM pollution events (for definition of PM pollution event see Section 3.3.2) during VAPE-likely conditions than VAPE-unlikely conditions (Table 3). We infer that the PM pollution events during intervals when the plume was likely to be absent were caused by non-volcanic sources such as cooking fires, agricultural fires, or wildfire events. Satellite-derived information is available regarding wildfire events in Nicaragua [NASA 2021], however smaller-scale events such as cooking fires, burning of household waste, and smaller-scale agricultural fires are not readily traceable. The PM pollution events during VAPE-unlikely conditions may also be caused by unsuccessful identification of plume presence by ECMWF data or satellite imagery (given the uncertainties as mentioned in Section 2.5.3 and Section 2.5.4).

The AQMesh pod at the Rigoberto measurement station had an insignificant difference between VAPE-likely and VAPE-unlikely conditions for all PM size fractions in the two-sample t-test. There was also a low variability in the frequency of PM pollution events between VAPE-likely and VAPE-unlikely conditions (Table 3). This is likely due to a coincidence of two factors. Rigoberto is located on the edge of the prevailing plume direction (Figure 2) and therefore is likely to receive a more dilute VAP with lower frequency of volcanic PM pollution events. The close proximity of the pod to domestic cooking fires was likely the more important source of the local PM pollution events, overriding the signal of VAP. These results highlight the importance of considering different air pollution sources together and not placing volcanic-pollution detection instruments in places likely to be impacted by non-volcanic pollution.

4.1.2 *Far-field locations impacted by the plume*

The AQMesh pods at the El Crucero and Pacaya measurement stations were the least efficient at recognising the presence of the volcanic plume using simultaneously elevated concentrations of SO_2 and PM, with only minimal volcanic signatures recorded at El Crucero and none at the Pacaya station. The inefficiency of this method may be related to the greater distance between the volcanic source and the measurement sites (16 km from the crater, as opposed to 4 km for the near-field stations). Firstly, the greater distance may re-

sult in higher uncertainty in identifying the plume dispersal direction through meteorological forecasts. The ECMWF data were extracted for the grid point local to Santiago Crater and may not be representative of wind conditions over the full distance between the volcanic source and the Las Sierras highlands. The downwind variability in wind direction was observed on several occasions in satellite imagery with non-linear dispersion of the volcanic plume (Figure 5A]. Additionally, although meteorological data may correctly suggest the plume is being dispersed towards a measurement station on a given day, these parameters do not guarantee that the plume will "ground" and be measurable at ground-level. It is noted that the assumed plume height of 948 m $\pm$ 112 m asl could yield plume altitude below the Las Sierras ridge at 925 m, potentially acting to block the plume, although plume has been detected on the ridge previously [Delmelle et al. 2002; Mather et al. 2003]. Secondly, over the 16 km distance between the volcanic source and the Las Sierras highlands, the plume may have become diluted into the atmosphere to the extent that the concentration was below the reliable range of the sensors. Thirdly, if in-plume conversion of SO_2 to PM was very extensive, this could eventually lower the correlation between SO_2 and PM. As such, the apparent inefficiency of the El Crucero and Pacaya AQMesh pods may be because the plume was not physically present at the stations at times when the ECMWF data and satellite imagery suggests it would be. Were the experiment to be repeated, it would be invaluable to set up a reference-grade measurement station for long-term monitoring alongside at least one of the far-field AQMesh stations. This would allow verification of the presence or absence of elevated SO_2 and PM at ground level and testing of the response of the AQMesh pod relative to the reference-grade instrument. In turn, this would allow verification of whether the AQMesh pods were correct in their positive or negative identification of the plume's presence. It would also be valuable to better constrain the plume height and extent in the vertical, potentially using drone or meteorological balloon measurements.

The PM distribution analysis at the El Crucero station indicated significantly higher frequencies of PM pollution events during VAPE-likely conditions than VAPE-unlikely conditions (Table 3), similar to that found at El Panama. At Pacaya AQMesh station the enhancement in VAPE-likely PM pollution events was lower than at El Crucero, in spite of the proximity of the two stations (Figure 2). The cause for the smaller difference between VAPE-likely and VAPE-unlikely conditions at Pacaya is uncertain, but may be a result of localised anthropogenic pollution sources. The Pacaya station was located on the roof of a clinic, possibly resulting in more traffic-related pollution during the day. This potentially demonstrates the small-scale variability in pollution levels.

4.1.3 *PM pollution events*

Based on the SO_2 flux from 2016 (Figure 1) and visual observations of the plume during our fieldwork in 2017, the emissions from Masaya were relatively low during the measurement period of this study. The frequency and concentration of the pollution events reported here should therefore be taken as a possible lower-limit at Masaya. Due to the high uncertainty in the quantitative measurements of SO_2 we refrain from discussing related air quality impacts, and focus on the PM data in this context. While the long-term average PM concentration is relatively low at all stations (Figure 9), the pollution events (both volcanic and non-volcanic) reach potentially unhealthy values (24-hour average: $PM_{2.5} > 35\,\mu g\,m^{-3}$ [EPA 2013]) and support the need for an operational air quality network. At both near- and far-field stations impacted by the plume, the VAP-related pollution events enhance the concentration of PM_1 and $PM_{2.5}$ to a greater extent than PM_{10}, consistent with the fine size of volcanic particulates [Martin et al. 2011; Ilyinskaya et al. 2017; 2021; Mason et al. 2021] (Table 3). This is important for the potential impacts of VAP as fine PM is associated with more detrimental effects on human health, morbidity, and mortality [Holgate 2017].

4.2 Alternative air quality monitoring tools

The AQMesh pods are a relatively low-cost monitoring option. A network of five AQMesh pods for permanent installation would have an initial cost of £35,000 (~US$48,000), as quoted from ACOEM Air Monitors in 2021, followed by yearly server and maintenance costs. They are easy to install and do not require a large amount of infrastructure to operate. However, they suffered from frequent instrument failure in this case study, presumably to be due to the high level of fast-acting corrosion from the volcanic plume (Figure 3). In such instances they require continual maintenance and purchase of replacement parts. Although having the advantage of being low-cost and relatively compact, the AQMesh instruments have the drawback of being less precise and accurate than larger reference-grade instruments, as indicated in Figure 7. The data from the instruments also requires substantial processing and analysis, meaning that the current set-up is not useful for plume monitoring in real time until automatic algorithms can be implemented.

In comparison, if a network of reference-grade monitoring instruments were installed, the cost of installation and construction of the required infrastructure would be significantly higher. A single pulsed fluorescence spectroscopy SO_2 analyser costs in the range of £8,000 to £12,000 (~US$10,900 to US$16,300) depending on the configuration (quote from Thermo Scientific [2010]). A BAM-1020 (manufactured by Met One Instruments) which is a reference-grade FEM in-

strument for measuring PM would cost in the range of £17,000 (~US$23,200) (quote from Enviro Technology Services Ltd, 2021). The instrumentation cost of one reference-grade monitoring station would therefore be in the range of £25,000 to £29,000 (~US$34,000 to ~US$39,500), and a network of five would be approximately £135,000 (~US$184,000) for instrument purchase alone. Permanent ambient air quality stations such as these must be kept in air-conditioned enclosures to maintain long-term stability, adding considerable additional cost and time considerations related to construction of buildings with access to mains power. Although such a network of reference-grade monitoring instruments would provide accurate and reliable measurements of volcanic plume in downwind locations, the feasibility of installing such a high-expense monitoring network is restricted where resources are more limited.

An alternative option for an even cheaper low-cost instrument network would be PurpleAir sensors. PurpleAir (Utah, USA) instruments cost approximately US$250 (~£180) per unit (quote from PurpleAir, 2019) and can be purchased and operated by members of the community with all data available online in an open-access, user-friendly format [PurpleAir 2019]. PurpleAir instruments only have the capability of measuring PM, which they measure using Plantower PMS5003 sensors [Kelly et al. 2017; Sayahi et al. 2019]. Each PurpleAir contains two Plantower PMS5003 sensors mounted in one housing, allowing self-consistency checks to alert when significant differences are reported between the internal sensors. The instruments are easy to install, though do require mains power and stable WiFi access. The data are uploaded automatically to the PurpleAir web server, removing the need for custom-made data infrastructure. The real-time map view allows the air quality to be interpreted by non-specialists with ease. During the 2018 eruption of Kīlauea's lower East Rift Zone on the Island of Hawai'i, PurpleAir instruments were installed across the island and provided an open-access source of air quality information with a high level of accuracy (Pearson's r value of 0.92) as compared to reference-grade PM sensors [Whitty et al. 2020].

A recent study by Crawford et al. [2021] deployed a network of low-cost sensors similar to the ones described here across the Island of Hawai'i to monitor Kīlauea's lower East Rift Zone in 2018. They used a combination of OPC-N2 sensors, as found in AQMesh pods, and Plantower PMS5003 sensors, as found in PurpleAir instruments, to measure PM variability across a large spatial area. Additionally, SO_2 was measured using Alphasense B4-series electrochemical sensors, as used in the AQMesh pods. The network consisted of 33 sensor nodes, deployed for a total of 17 days during July to August 2018. The PM measurements were corrected for the effect of high humidity. Similar to this six-month study, in several of the network nodes Crawford et al. [2021] found SO_2 sensors to experience technical difficulties over the 17-day deployment period. The results from this combined-sensor low-cost network were successful, with similar PM and SO_2 measurements recorded as the regulatory reference-grade network and at a much higher spatial resolution [Crawford et al. 2021]. Crawford et al. [2021] do not report on the performance of the network over long-term deployment so it is not possible to make a direct comparison with that of the AQMesh network at Masaya.

In a downwind volcanic setting, such as that surrounding Masaya volcano, conditions can be challenging for air quality monitoring networks, especially with the added complications of a warm and humid meteorological climate. In such settings it is necessary to consider the balance between a monitoring network's ability to generate accurate and reliable measurements against its financial cost, both for the initial installation of the network, and the on-going burden of instrument maintenance. In Global South countries such as Nicaragua, limited resources and infrastructure may determine that the financial burden of installing a full-scale reference-grade monitoring network is too high. In such instances, governmental bodies and researchers must weigh up the benefits and disadvantages of alternative monitoring networks at lower costs while attempting to develop a monitoring system which achieves the primary goal of effectively monitoring air quality and disseminating the information to local exposed communities. For the area impacted by Masaya volcano (and comparable areas elsewhere), we conclude that a combined monitoring approach is the one most likely to achieve this primary goal. The resources required would be for the installation and maintenance of one reference-grade monitoring station (consisting of FEM-approved instrumentation for monitoring of SO_2 and PM) and a network of lower-cost instruments to provide a higher spatial resolution. The continuous highly-accurate measurements from the reference-grade station would provide a reliable point-location determination of the daily concentration of SO_2 and PM, allowing residents to determine the potential likely health-impacts from the volcanic-induced air quality. The reference-grade monitoring station would also be used for regular calibrations of the lower-cost instruments under local atmospheric (ambient temperature, relative humidity, etc.) and environmental conditions (concentration and type of pollutants), including following maintenance and sensor replacements for the lower-cost instruments. The location of the reference-grade station would be strategically selected depending on a) how likely it is to be impacted by the volcanic plume on a regular basis, b) how representative it is for local population exposure, and c) how accessible it is for network maintenance, including the regular calibrations of the lower-cost instruments. We suggest that downwind of Masaya volcano, a reference-grade monitoring station installed

in El Panama would fulfil these requirements. The type of lower-cost instruments that are to be selected for the network have to be carefully considered because, as shown in this work, they can be subject to frequent component failures which may result in significant total costs. Based on our results, we suggest that AQMesh pods (or comparable gas-sensing instruments from other manufacturers) would require some modifications and subsequent testing in a volcanic environment if they are to be used for permanent monitoring in order to reduce downtime due to component failures. The necessary modifications would include better insulation of the internal electronics (Section 4.3), which we found to corrode quickly in areas that are more exposed to the volcanic plume. PurpleAir PM-only sensors have been shown to be suitable for long-term deployment (three month duration) in the far-field volcanic environment on the Island of Hawai'i [Whitty et al. 2020], and we suggest that they may be a suitable instrument type for the far-field areas downwind of Masaya, which receive relatively low concentrations of SO_2 (considering the current SO_2 flux) but higher PM concentrations. The proposed combined network, at a medium cost level, would provide good spatial coverage across the exposed area and allow real-time information dissemination to exposed communities. The data accuracy would vary between the reference-grade and the lower-cost instruments but the ability to locally calibrate the lower-grade instruments would reduce uncertainty.

4.3 Recommendations for future use of low-cost sensor systems around Masaya volcano

Were the AQMesh pods to be installed as permanent monitoring stations in a volcanic environment similar to the region downwind of Masaya volcano, there are several practical measures that could be implemented to increase the effectiveness of the instruments to detect the plume and yield more quantitative data on air quality and plume exposure. The main issue faced during this deployment was the fast-acting high level of corrosion resulting from the volcanic environment. Where feasible this could be at least partially mitigated by shielding of exposed metal components within the AQMesh pods and circuit boards using protective coatings such as epoxy, aerosol spray, and solder masks to coat vulnerable components and minimise exposure to corrosion [González-García et al. 2007; Liu et al. 2009]. This could improve the time-coverage and quantitative nature of the network measurements, by reducing the need to replace sensors, and thereby enabling a more detailed sensor characterisation and cross-calibration of sensors from the network pods to reference-grade SO_2 and PM instruments. Further to this, if infrastructure were implemented to allow the AQMesh pods to be connected to mains power, this would remove the need for battery re-charging every four weeks, therefore reducing both the maintenance time and costs as well as reducing instances of the instruments being offline when recharging was delayed.

On-site measurements of humidity are crucial to allow effective correction of the PM counts [Crilley et al. 2018; 2020]. Humidity measurements are also important to allow filtering of the SO_2 measurements by the electrochemical sensors: this study focused on measurement intervals where sensors reported $SO_2 > 20$ ppbv because at low SO_2 abundances a diurnal signal with high correlation between recorded SO_2 and humidity might indicate a sensor response due to environmental conditions and not true SO_2 concentrations. Where funds and infrastructure allow, installation of a meteorological station at a suitable site close to the volcanic source (perhaps upwind to minimise corrosion) would also be invaluable to allow identification of local wind conditions and direction of plume dispersal on a real-time basis, as would methods to better constrain the plume height.

4.4 Volcanic air pollution exposure mitigation

Exposure to volcanic SO_2 and PM can cause long-term health impacts and result in significant issues, particularly for children and vulnerable individuals including people with asthma [ATSDR 1998; CRI 2004]. In the communities downwind of persistently degassing volcanoes, like Masaya, exposure can be ongoing over years. Depending on the rate of volcanic degassing, the meteorological conditions and the characteristics of the plume, exposure to volcanic SO_2 and PM in any one location fluctuates, as shown in this study and by previous reports. If there is adequate monitoring of volcanic SO_2 and/or PM concentrations in downwind communities, the residents can react to the fluctuating presence of the plume. During periods of extreme degassing from Kīlauea volcano in Hawai'i in 2018, official government advice included remaining indoors, closing doors and windows and recirculating air within buildings [Hawaii Emergency Management Agency 2018]. In low-latitude Global South countries such as Nicaragua, buildings are not commonly airtight and so mitigation strategies would focus more on avoiding excessive physical activity during especially high levels of exposure [Pohl 1998; Williams-Jones and Rymer 2015; IVHHN 2020]. Highly vulnerable individuals may be advised to leave the affected area during extreme VAPE. These mitigation strategies work best when there is clear communication to the public regarding the concentration of volcanic SO_2 and PM that they are being exposed to in real-time. This most effectively works either with a well-maintained ground-based monitoring network with readily-accessible real-time data, or with a model forecast capable of accurately predicting the movement of the volcanic plume and allowing communication to community members of their level of volcanic exposure on any given day. Although the AQMesh network temporarily installed by the UNRESP project

in Nicaragua was not able to provide a real-time warning system, it demonstrated that it would be highly beneficial to the communities surrounding the volcano for an operational monitoring and/or forecasting system to be implemented.

5 Conclusions

A network of five AQMesh pods was installed in Nicaragua by the UNRESP project between February and August 2017. The network data were analysed to assess the pods' effectiveness at recognising the presence of volcanic plume at the measurement stations. Intervals where volcanic plume was likely to have been present at measurement stations were assessed from ECMWF meteorological forecasts and from visual inspection of visible plume extension seen in high-resolution satellite imagery. The data from the AQMesh pods were analysed to identify volcanic signatures by simultaneous enhancement of SO_2 and PM_1, $PM_{2.5}$, and PM_{10}, respectively. The PM data were also analysed separately to determine differences in the size distribution and concentration of particles under VAPE-likely and VAPE-unlikely conditions.

The near-field stations of El Panama and Rigoberto were reasonably effective at positively identifying the presence of the volcanic plume using simultaneous enhancement of SO_2 and PM during periods when meteorological data indicated plume dispersal towards the measurement station. Both these AQMesh sites measured plume more often during VAPE-likely periods (61 % of the time for SO_2 and $PM_{2.5}$ at El Panama and 41 % of the time for SO_2 and $PM_{2.5}$ at Rigoberto) than during VAPE-unlikely periods (23 % of the time for SO_2 and $PM_{2.5}$ at El Panama and 15 % of the time for SO_2 and $PM_{2.5}$ at Rigoberto). The far-field stations of El Crucero and Pacaya were least effective at identifying the plume's presence via means of simultaneous enhancement of SO_2 and PM. No SO_2 to PM enhancement were identified from data collected at the Pacaya station, and El Crucero's AQMesh pod positively identified the presence of the plume only 4 % of the time during VAPE-likely intervals, with an equal occurrence of plume when it was indicated to be absent. The inefficiency of the El Crucero and Pacaya stations may be a result of the larger distance from the volcanic source, providing a greater potential for bias in the determination of VAPE-likely periods from meteorological conditions.

Analysis of the PM data indicated that both near-field and far-field stations can be suitable for identifying an increase in daily average PM during VAPE-likely conditions. The El Panama station recorded exceedance events above the background norm 40 % of the measurement time for $PM_{2.5}$ under VAPE-likely conditions, as opposed to 21 % of the time for VAPE-unlikely conditions. El Crucero similarly had a higher frequency of exceeding the background norm under VAPE-likely conditions (48 % for $PM_{2.5}$) as opposed to VAPE-unlikely conditions (5.5 % for $PM_{2.5}$). However, both the Pacaya and Rigoberto measurement stations showed small variations in the exceedances above background norms (25 % for VAPE-likely $PM_{2.5}$ periods and 20 % for VAPE-unlikely $PM_{2.5}$ periods at Pacaya, and 14 % for VAPE-likely $PM_{2.5}$ periods and 16 % for VAPE-unlikely $PM_{2.5}$ periods at Rigoberto). At Rigoberto the small variations in exceedances above background PM concentrations is suggested to be caused by the reasonably close proximity to domestic cooking fires, and that it is located at the edge of the zone most impacted by the prevailing plume dispersion. With PM analysis it appears very important to have a strong understanding of the other pollution sources. As such, the AQMesh pods are suitable for monitoring the presence of volcanic plume if it is possible to carefully site them to avoid other sources of contamination and if they are able to be frequently maintained to replace failed sensors.

The AQMesh pods that were installed in Nicaragua were originally designed for monitoring air quality in urban and commercial environments, and were severely affected by the volcanic environment in this study. All AQMesh pods required replacement parts to be installed, likely due to instrument failure or corrosion of key components, and there was a high frequency of AQMesh pods going offline. The AQMesh pods provide a relatively low-cost opportunity for monitoring volcanic gas and PM downwind from Masaya volcano, in comparison to reference-grade instrument networks. However, we propose a combined monitoring network approach that utilises a strategically-placed reference-grade monitoring station, supplemented by a wider network of low-cost instrument nodes. Countries with persistently outgassing volcanoes could greatly benefit from installation of permanent monitoring networks to track volcanic plume presence in downwind communities in real-time, together with the relevant information flow to communicate this information to vulnerable communities.

Acknowledgements

The authors would like to thank the communities of El Panama, Rigoberto, San Juan de La Concepción, Pacaya and El Crucero in Nicaragua where the AQMesh pods were installed. The UNRESP team dedicates this work to the memory of Dr. Caroline Williams, University of Bristol.

RCWW is funded by the Leeds-York Natural Environment Research Council (NERC) Doctoral Training Partnership (DTP) NE/L002574/1, in CASE partnership with the Icelandic Meteorological Office. TJR acknowledges ANR Projet de Recherche Collaborative VOLC-HAL-CLIM (Volcanic Halogens: from Deep

Earth to Atmospheric Impacts), ANR-18-CE01-11. IAT acknowledges the support of the Centre for Observation and Modelling of Earthquakes, Volcanoes and Tectonics (COMET) and NERC funding through the Oxford Environmental Research DTP (NE/L002612/1). The "Unseen but not unfelt: resilience to persistent volcanic emissions (UNRESP)" project was funded by GCRF NE/P015271/1 and NE/R009465/1.

Author contributions

RCWW performed the data analysis and wrote the original draft. MAP, EI, TJR, TAM contributed to data interpretation and manuscript drafting. EI was the principal investigator of UNRESP and developed the project idea with SN, XHL, PB, SB, WS, DL, HF, TAM and AS. WS advised on and, together with EI, coordinated the work in Nicaragua. EI, HB, EM, NP, IAT, PB, EJL, TAM and RCWW collected the field data through network set-up and maintenance. LRC and FDP contributed to PM humidity correction. SB and AS contributed to ECMWF forecast data. All co-authors contributed to draft review and editing.

Author affiliations

α Institute of Geophysics and Tectonics, School of Earth and Environment, University of Leeds, Leeds, United Kingdom.
β Icelandic Meteorological Office, Reykjavik, Iceland.
γ CNRS UMR7328, Laboratoire de Physique et de Chimie de l'Environnement et de l'Espace, Université d'Orléans, Orléans, France.
δ Department of Geography, University of Cambridge, Cambridge, United Kingdom.
ϵ Department of Chemistry, University of Cambridge, Cambridge, United Kingdom.
ζ Instituto Nicaragüense de Estudios Territoriales (INETER), Managua, Nicaragua.
η Department of Chemistry, York University, Toronto, Canada.
θ School of Geography, Earth and Environmental Sciences, University of Birmingham, Birmingham, United Kingdom.
ι Department of Geography, University of Montreal, Quebec, Canada.
κ Department of Earth Sciences, University of Oxford, Oxford, United Kingdom.
λ Department of Earth Sciences, University College London, London, United Kingdom.
μ Department of Electronic and Electrical Engineering, University College London, London, United Kingdom.
ν COMET, Atmospheric, Oceanic and Planetary Physics, University of Oxford, Oxford, United Kingdom.
ξ Department of Humanities, University of Northumbria, Newcastle, United Kingdom.
o Independent social research consultant.
π Cultural Institute, University of Leeds, Leeds, United Kingdom.
ρ Sustainability Research Institute, University of Leeds, Leeds, United Kingdom.
ς Department of Public Health and Primary Care, University of Cambridge, Cambridge, United Kingdom.

Data availability

The datasets analysed for this study can be found on figshare at DOI: 10.6084/m9.figshare.14916543.

Copyright notice

References

Agency for Toxic Substances and Disease Registry (ATSDR) (1998). "Public health statement Sulfur Dioxide". [CAS#: 7446-09-5].

Aiuppa, A., J. M. de Moor, S. Arellano, D. Coppola, V. Francofonte, B. Galle, G. Giudice, M. Liuzzo, E. Mendoza, A. Saballos, et al. (2018). "Tracking formation of a lava lake from ground and space: Masaya volcano (Nicaragua), 2014–2017". *Geochemistry, Geophysics, Geosystems* 19(2), pp. 496–515. DOI: 10.1002/2017GC007227.

Allen, A. G., C. Oppenheimer, M. Ferm, P. Baxter, L. A. Horrocks, B. Galle, A. McGonigle, and H. Duffell (2002). "Primary sulfate aerosol and associated emissions from Masaya Volcano, Nicaragua". *Journal of Geophysical Research: Atmospheres* 107(D23), ACH–5. DOI: 10.1029/2002JD002120.

Allen, A., T. Mather, A. McGonigle, A. Aiuppa, P. Delmelle, B. Davison, N. Bobrowski, C. Oppenheimer, D. Pyle, and S. Inguaggiato (2006). "Sources, size distribution, and downwind grounding of aerosols from Mount Etna". *Journal of Geophysical Research: Atmospheres* 111(D10). DOI: 10.1029/2005JD006015.

Alphasense (2021). *SO2-B4 Sulfur Dioxide Sensor Data Sheet*. URL: https://www.alphasense.com/wp-content/uploads/2019/09/SO2-B4.pdf (visited on 05/02/2021).

AQMesh (2017a). *Data Access*. URL: https://www.aqmesh.com/products/data-access/ (visited on 02/27/2021).

– (2017b). *Technical Specifications*. URL: %5Curl%7Bhttps://www.aqmesh.com/products/technical-specification/%7D (visited on 02/27/2021).

Austin, C. C., B. Roberge, and N. Goyer (2006). "Cross-sensitivities of electrochemical detectors used to monitor worker exposures to airborne contaminants: False positive responses in the absence of target analytes". *Journal of Environmental Monitoring* 8(1), pp. 161–166. doi: 10.1039/B510084D.

Baxter, P. J., R. E. Stoiber, and S. N. Williams (1982). "Volcanic gases and health: Masaya volcano, Nicaragua". *The Lancet* 320(8290), pp. 150–151. doi: 10.1016/s0140-6736(82)91109-6.

Buizza, R., P. Houtekamer, G. Pellerin, Z. Toth, Y. Zhu, and M. Wei (2005). "A comparison of the ECMWF, MSC, and NCEP global ensemble prediction systems". *Monthly Weather Review* 133(5), pp. 1076–1097. doi: 10.1175/MWR2905.1.

Burton, M. R., C. Oppenheimer, L. A. Horrocks, and P. W. Francis (2000). "Remote sensing of CO2 and H2O emission rates from Masaya volcano, Nicaragua". *Geology* 28(10), p. 915. doi: 10.1130/0091-7613(2000)28<915:rsocah>2.0.co;2.

Butwin, M. K., S. von Löwis, M. A. Pfeffer, and T. Thorsteinsson (2019). "The effects of volcanic eruptions on the frequency of particulate matter suspension events in Iceland". *Journal of Aerosol Science* 128, pp. 99–113. doi: 10.1016/j.jaerosci.2018.12.004.

Cadle, R., A. Wartburg, and P. Grahek (1971). "The proportion of sulfate to sulfur dioxide in Kilauea Volcano fume". *Geochimica et Cosmochimica Acta* 35(5), pp. 503–507. doi: 10.1016/0016-7037(71)90046-9.

Carlsen, H. K., E. Ilyinskaya, P. J. Baxter, A. Schmidt, T. Thorsteinsson, M. A. Pfeffer, S. Barsotti, F. Dominici, R. G. Finnbjornsdottir, T. Jóhannsson, T. Aspelund, T. Gislason, U. Valdimarsdóttir, H. Briem, and T. Gudnason (2021a). "Increased respiratory morbidity associated with exposure to a mature volcanic plume from a large Icelandic fissure eruption". *Nature Communications* 12(1). doi: 10.1038/s41467-021-22432-5.

Carlsen, H. K., U. Valdimarsdóttir, H. Briem, F. Dominici, R. G. Finnbjornsdottir, T. Jóhannsson, T. Aspelund, T. Gislason, and T. Gudnason (2021b). "Severe volcanic SO_2 exposure and respiratory morbidity in the Icelandic population – a register study". *Environmental Health* 20(1). doi: 10.1186/s12940-021-00698-y.

Cohen, A. J., H. R. Anderson, B. Ostro, K. D. Pandey, M. Krzyzanowski, N. Künzli, K. Gutschmidt, A. Pope, I. Romieu, J. M. Samet, and K. Smith (2005). "The Global Burden of Disease Due to Outdoor Air Pollution". *Journal of Toxicology and Environmental Health, Part A* 68(13-14), pp. 1301–1307. doi: 10.1080/15287390590936166.

Crawford, B., D. H. Hagan, I. Grossman, E. Cole, L. Holland, C. L. Heald, and J. H. Kroll (2021). "Mapping pollution exposure and chemistry during an extreme air quality event (the 2018 Kīlauea eruption) using a low-cost sensor network". *Proceedings of the National Academy of Sciences* 118(27), e2025540118. doi: 10.1073/pnas.2025540118.

Crilley, L. R., M. Shaw, R. Pound, L. J. Kramer, R. Price, S. Young, A. C. Lewis, and F. D. Pope (2018). "Evaluation of a low-cost optical particle counter (Alphasense OPC-N2) for ambient air monitoring". *Atmospheric Measurement Techniques* 11(2), pp. 709–720. doi: 10.5194/amt-11-709-2018.

Crilley, L. R., A. Singh, L. J. Kramer, M. D. Shaw, M. S. Alam, J. S. Apte, W. J. Bloss, L. H. Ruiz, P. Fu, W. Fu, S. Gani, M. Gatari, E. Ilyinskaya, A. C. Lewis, D. Ng'ang'a, Y. Sun, R. C. W. Whitty, S. Yue, S. Young, and F. D. Pope (2020). "Effect of aerosol composition on the performance of low-cost optical particle counter correction factors". *Atmospheric Measurement Techniques* 13(3), pp. 1181–1193. doi: 10.5194/amt-13-1181-2020.

Delmelle, P., J. Stix, P. Baxter, J. Garcia-Alvarez, and J. Barquero (2002). "Atmospheric dispersion, environmental effects and potential health hazard associated with the low-altitude gas plume of Masaya volcano, Nicaragua". *Bulletin of Volcanology* 64(6), pp. 423–434. doi: 10.1007/s00445-002-0221-6.

Delmelle, P., P. Baxter, A. Beaulieu, M. Burton, P. Francis, J. Garcia-Alvarez, L. Horrocks, M. Navarro, C. Oppenheimer, D. Rothery, H. Rymer, K. S. Amand, J. Stix, W. Strauch, and G. Williams-Jones (1999). "Origin, effects of Masaya Volcano's continued unrest probed in Nicaragua". *Eos, Transactions American Geophysical Union* 80(48), p. 575. doi: 10.1029/eo080i048p00575.

Duffell, H. J., C. Oppenheimer, D. M. Pyle, B. Galle, A. J. McGonigle, and M. R. Burton (2003). "Changes in gas composition prior to a minor explosive eruption at Masaya volcano, Nicaragua". *Journal of Volcanology and Geothermal Research* 126(3-4), pp. 327–339. doi: 10.1016/s0377-0273(03)00156-2.

Environmental Protection Agency (EPA) (2010). *Primary National Ambient Air Quality Standard for Sulfur Dioxide; Final Rule*. url: https://www.govinfo.gov/content/pkg/FR-2010-06-22/pdf/2010-13947.pdf (visited on 01/15/2019).

– (2013). *Federal and State Ambient Air Quality Standards*. url: http://health.hawaii.gov/cab/files/2013/05/naaqs_jan_2013.pdf (visited on 01/15/2019).

– (2016). *List of designated reference and equivalent methods*. url: https://www.epa.gov/sites/production/files/2019-08/documents/designated_reference_and-equivalent_methods.pdf (visited on 01/15/2019).

Galle, B., C. Oppenheimer, A. Geyer, A. J. S. McGonigle, M. Edmonds, and L. Horrocks (2003). "A miniaturised ultraviolet spectrometer for remote sensing of SO_2 fluxes: a new tool for volcano surveillance". *Journal of Volcanology and Geothermal Research* 119(1-4), pp. 241–254. doi: 10.1016/s0377-0273(02)00356-6.

Gao, X., B. Coull, X. Lin, P. Vokonas, A. Spiro, L. Hou, J. Schwartz, and A. A. Baccarelli (2021). "Short-term air pollution, cognitive performance and nonsteroidal anti-inflammatory drug use in the Veterans Affairs Normative Aging Study". *Nature Aging* 1(5), pp. 430–437. DOI: 10.1038/s43587-021-00060-4.

Global Volcanism Program (2021). "Report on Masaya (Nicaragua)". *Bulletin of the Global Volcanism Network* 46(6). Ed. by K. L. Bennis and E. Venzke. DOI: 10.5479/si.gvp.bgvn202106-344100.

González-García, Y., S. González, and R. Souto (2007). "Electrochemical and structural properties of a polyurethane coating on steel substrates for corrosion protection". *Corrosion Science* 49(9), pp. 3514–3526. DOI: 10.1016/j.corsci.2007.03.018.

Gysel, M., J. Crosier, D. O. Topping, J. D. Whitehead, K. N. Bower, M. J. Cubison, P. I. Williams, M. J. Flynn, G. B. McFiggans, and H. Coe (2007). "Closure study between chemical composition and hygroscopic growth of aerosol particles during TORCH2". *Atmospheric Chemistry and Physics* 7(24), pp. 6131–6144. DOI: 10.5194/acp-7-6131-2007.

Hagan, D. H., G. Isaacman-VanWertz, J. P. Franklin, L. M. M. Wallace, B. D. Kocar, C. L. Heald, and J. H. Kroll (2018). "Calibration and assessment of electrochemical air quality sensors by co-location with regulatory-grade instruments". *Atmospheric Measurement Techniques* 11(1), pp. 315–328. DOI: 10.5194/amt-11-315-2018.

Hawaii Emergency Management Agency (2018). *How to cope with hazardous volcanic gas emissions*. URL: http://dod.hawaii.gov/hiema/how-to-cope-with-hazardous-volcanic-gas-emissions (visited on 04/15/2021).

Holgate, S. T. (2017). "'Every breath we take: the lifelong impact of air pollution' – a call for action". *Clinical Medicine* 17(1), pp. 8–12. DOI: 10.7861/clinmedicine.17-1-8.

Ilyinskaya, E., C. Oppenheimer, T. A. Mather, R. S. Martin, and P. R. Kyle (2010). "Size-resolved chemical composition of aerosol emitted by Erebus volcano, Antarctica". *Geochemistry, Geophysics, Geosystems* 11(3). DOI: 10.1029/2009gc002855.

Ilyinskaya, E., E. Mason, P. E. Wieser, L. Holland, E. J. Liu, T. A. Mather, M. Edmonds, R. C. W. Whitty, T. Elias, P. A. Nadeau, D. Schneider, J. B. McQuaid, S. E. Allen, J. Harvey, C. Oppenheimer, C. Kern, and D. Damby (2021). "Rapid metal pollutant deposition from the volcanic plume of Kīlauea, Hawai'i". *Communications Earth & Environment* 2(1). DOI: 10.1038/s43247-021-00146-2.

Ilyinskaya, E., A. Schmidt, T. A. Mather, F. D. Pope, C. Witham, P. Baxter, T. Jóhannsson, M. Pfeffer, S. Barsotti, A. Singh, P. Sanderson, B. Bergsson, B. M. Kilbride, A. Donovan, N. Peters, C. Oppenheimer, and M. Edmonds (2017). "Understanding the environmental impacts of large fissure eruptions: Aerosol and gas emissions from the 2014–2015 Holuhraun eruption (Iceland)". *Earth and Planetary Science Letters* 472, pp. 309–322. DOI: 10.1016/j.epsl.2017.05.025.

International Volcanic Health Hazard Network (IVHHN) (2020). *The health hazards of volcanic and geothermal gases: A guide for the public*. URL: https://www.ivhhn.org/information/health-impacts-volcanic-gases%5C#Howtolivewithvolcanicemissions (visited on 04/12/2021).

Jayaratne, R., X. Liu, P. Thai, M. Dunbabin, and L. Morawska (2018). "The influence of humidity on the performance of a low-cost air particle mass sensor and the effect of atmospheric fog". *Atmospheric Measurement Techniques* 11(8), pp. 4883–4890. DOI: 10.5194/amt-11-4883-2018.

Kelly, K. E., J. Whitaker, A. Petty, C. Widmer, A. Dybwad, D. Sleeth, R. Martin, and A. Butterfield (2017). "Ambient and laboratory evaluation of a low-cost particulate matter sensor". *Environmental Pollution* 221, pp. 491–500. DOI: 10.1016/j.envpol.2016.12.039.

Krogh, A. (2019). *Snazzy Maps*. URL: https://snazzymaps.com/ (visited on 01/20/2021).

Lambert, G., M.-F. L. Cloarec, and M. Pennisi (1988). "Volcanic output of SO_2 and trace metals: A new approach". *Geochimica et Cosmochimica Acta* 52(1), pp. 39–42. DOI: 10.1016/0016-7037(88)90054-3.

Langmann, B. (2014). "On the Role of Climate Forcing by Volcanic Sulphate and Volcanic Ash". *Advances in Meteorology* 2014, pp. 1–17. DOI: 10.1155/2014/340123.

Lewis, A. C., J. D. Lee, P. M. Edwards, M. D. Shaw, M. J. Evans, S. J. Moller, K. R. Smith, J. W. Buckley, M. Ellis, S. R. Gillot, and A. White (2016). "Evaluating the performance of low cost chemical sensors for air pollution research". *Faraday Discussions* 189, pp. 85–103. DOI: 10.1039/c5fd00201j.

Li, Z., N. Marston, and K. Stokes (2018). *Materials within geothermal environments*. Judgeford, New Zealand: BRANZ Ltd. BRANZ study report SR393.

Lim, S. S. et al. (2012). "A comparative risk assessment of burden of disease and injury attributable to 67 risk factors and risk factor clusters in 21 regions, 1990–2010: a systematic analysis for the Global Burden of Disease Study 2010". *The Lancet* 380(9859), pp. 2224–2260. DOI: 10.1016/s0140-6736(12)61766-8.

Liu, X., J. Xiong, Y. Lv, and Y. Zuo (2009). "Study on corrosion electrochemical behavior of several different coating systems by EIS". *Progress in Organic Coatings* 64(4), pp. 497–503. DOI: 10.1016/j.porgcoat.2008.08.012.

Longo, B. M., A. Rossignol, and J. B. Green (2008). "Cardiorespiratory health effects associated with sulphurous volcanic air pollution". *Public Health* 122(8), pp. 809–820. DOI: 10.1016/j.puhe.2007.09.017.

Longo, B. M. (2013). "Adverse Health Effects Associated with Increased Activity at Kīlauea Volcano: A Repeated Population-Based Survey". *ISRN Public Health* 2013, pp. 1–10. doi: 10.1155/2013/475962.

Loughlin, S., W. Aspinall, C. Vye-Brown, P. Baxter, C. Braban, M. Hort, A. Schmidt, T. Thordarson, and C. Witham (2012). "Large-magnitude fissure eruptions in Iceland: source characterisation". *BGS Open File Report* OR/12/098(OR/12/098).

Martin, R. S., E. Ilyinskaya, G. M. Sawyer, V. I. Tsanev, and C. Oppenheimer (2011). "A re-assessment of aerosol size distributions from Masaya volcano (Nicaragua)". *Atmospheric Environment* 45(3), pp. 547–560. doi: 10.1016/j.atmosenv.2010.10.049.

Mason, E., P. E. Wieser, E. J. Liu, M. Edmonds, E. Ilyinskaya, R. C. W. Whitty, T. A. Mather, T. Elias, P. A. Nadeau, T. C. Wilkes, A. J. S. McGonigle, T. D. Pering, F. M. Mims, C. Kern, D. J. Schneider, and C. Oppenheimer (2021). "Volatile metal emissions from volcanic degassing and lava–seawater interactions at Kīlauea Volcano, Hawai'i". *Communications Earth & Environment* 2(1). doi: 10.1038/s43247-021-00145-3.

Mather, T. ., D. M. Pyle, V. I. Tsanev, A. J. S. McGonigle, C. Oppenheimer, and A. G. Allen (2006a). "A reassessment of current volcanic emissions from the Central American arc with specific examples from Nicaragua". *Journal of Volcanology and Geothermal Research* 149(3-4), pp. 297–311. doi: 10.1016/j.jvolgeores.2005.07.021.

Mather, T. A., A. G. Allen, C. Oppenheimer, D. M. Pyle, and A. J. S. McGonigle (2003). *Journal of Atmospheric Chemistry* 46(3), pp. 207–237. doi: 10.1023/a:1026327502060.

Mather, T. A., J. R. McCabe, V. K. Rai, M. H. Thiemens, D. M. Pyle, T. H. E. Heaton, H. J. Sloane, and G. R. Fern (2006b). "Oxygen and sulfur isotopic composition of volcanic sulfate aerosol at the point of emission". *Journal of Geophysical Research* 111(D18). doi: 10.1029/2005jd006584.

Mather, T. A. (2015). "Volcanoes and the environment: Lessons for understanding Earth's past and future from studies of present-day volcanic emissions". *Journal of Volcanology and Geothermal Research* 304, pp. 160–179. doi: 10.1016/j.jvolgeores.2015.08.016.

McBirney, A. R. (1956). "The Nicaraguan volcano Masaya and its caldera". *Transactions, American Geophysical Union* 37(1), p. 83. doi: 10.1029/tr037i001p00083.

McFiggans, G., M. R. Alfarra, J. Allan, K. Bower, H. Coe, M. Cubison, D. Topping, P. Williams, S. Decesari, C. Facchini, and S. Fuzzi (2005). "Simplification of the representation of the organic component of atmospheric particulates". *Faraday Discussions* 130, p. 341. doi: 10.1039/b419435g.

Mead, M. I., O. A. M. Popoola, G. B. Stewart, P. Landshoff, M. Calleja, M. Hayes, J. J. Baldovi, M. W. McLeod, T. F. Hodgson, J. Dicks, A. Lewis, J. Cohen, R. Baron, J. R. Saffell, and R. L. Jones (2013). "The use of electrochemical sensors for monitoring urban air quality in low-cost, high-density networks". *Atmospheric Environment* 70, pp. 186–203. doi: 10.1016/j.atmosenv.2012.11.060.

Miller, V. (2004). "Health Effects of Project SHAD Chemical Agent: Sulfur Dioxide", pp. 1–58.

Molteni, F., R. Buizza, T. N. Palmer, and T. Petroliagis (1996). "The ECMWF Ensemble Prediction System: Methodology and validation". *Quarterly Journal of the Royal Meteorological Society* 122(529), pp. 73–119. doi: 10.1002/qj.49712252905.

Nadeau, P. A. and G. Williams-Jones (2009). "Apparent downwind depletion of volcanic SO_2 flux—lessons from Masaya Volcano, Nicaragua". *Bulletin of Volcanology* 71(4), pp. 389–400. doi: 10.1007/s00445-008-0251-9.

National Aeronautics and Space Administration (NASA) (2021). *Fire Information for Resource Management System*. url: https://firms.modaps.eosdis.nasa.gov/map/#t:adv;d:2021-05-18..2021-05-19;@-85.7,11.9,10z (visited on 06/02/2021).

Oppenheimer, C. and A. J. S. McGonigle (2009). "Exploiting ground-based optical sensing technologies for volcanic gas surveillance". *Annals of Geophysics* 47(4). doi: 10.4401/ag-3353.

Oppenheimer, C., P. Francis, and J. Stix (1998). "Depletion rates of sulfur dioxide in tropospheric volcanic plumes". *Geophysical Research Letters* 25(14), pp. 2671–2674. doi: 10.1029/98gl01988.

Pattantyus, A. K., S. Businger, and S. G. Howell (2018). "Review of sulfur dioxide to sulfate aerosol chemistry at Kīlauea Volcano, Hawai'i". *Atmospheric Environment* 185, pp. 262–271. doi: 10.1016/j.atmosenv.2018.04.055.

Petters, M. D. and S. M. Kreidenweis (2007). "A single parameter representation of hygroscopic growth and cloud condensation nucleus activity". *Atmospheric Chemistry and Physics* 7(8), pp. 1961–1971. doi: 10.5194/acp-7-1961-2007.

Pfeffer, M. A., B. Langmann, and H.-F. Graf (2006a). "Atmospheric transport and deposition of Indonesian volcanic emissions". *Atmospheric Chemistry and Physics* 6(9), pp. 2525–2537. doi: 10.5194/acp-6-2525-2006.

Pfeffer, M., F. Rietmeijer, A. Brearley, and T. Fischer (2006b). "Electron microbeam analyses of aerosol particles from the plume of Poás Volcano, Costa Rica and comparison with equilibrium plume chemistry modeling". *Journal of Volcanology and Geothermal Research* 152(1-2), pp. 174–188. doi: 10.1016/j.jvolgeores.2005.10.009.

Pohl, H. R. (1998). *Toxicological profile for sulfur dioxide*. url: https://www.atsdr.cdc.gov/toxprofiles/tp116.pdf (visited on 01/10/2022).

Pringle, K. J., H. Tost, A. Pozzer, U. Pöschl, and J. Lelieveld (2010). "Global distribution of the effective aerosol hygroscopicity parameter for CCN activation". *Atmospheric Chemistry and Physics* 10(12), pp. 5241–5255. DOI: 10.5194/acp-10-5241-2010.

PurpleAir (2019). *PurpleAir: Air Quality Monitoring*. URL: https://www.purpleair.com/ (visited on 10/26/2018).

Read, K. (2018). *Report of Calibration Work*. URL: https://github.com/ncasuk/ncas-cozi-lab-additionaldata/blob/main/20180117_Certificate_SO2_43I_TRACE.pdf (visited on 01/10/2022).

Roberts, T. J., C. F. Braban, C. Oppenheimer, R. S. Martin, R. A. Freshwater, D. H. Dawson, P. T. Griffiths, R. A. Cox, J. R. Saffell, and R. L. Jones (2012). "Electrochemical sensing of volcanic gases". *Chemical Geology* 332-333, pp. 74–91. DOI: 10.1016/j.chemgeo.2012.08.027.

Roberts, T. J., D. Vignelles, M. Liuzzo, G. Giudice, A. Aiuppa, M. Coltelli, G. Salerno, M. Chartier, B. Couté, G. Berthet, T. Lurton, F. Dulac, and J.-B. Renard (2018). "The primary volcanic aerosol emission from Mt Etna: Size-resolved particles with SO_2 and role in plume reactive halogen chemistry". *Geochimica et Cosmochimica Acta* 222, pp. 74–93. DOI: 10.1016/j.gca.2017.09.040.

Rotstayn, L. D. and U. Lohmann (2002). "Simulation of the tropospheric sulfur cycle in a global model with a physically based cloud scheme". *Journal of Geophysical Research: Atmospheres* 107(D21), AAC 20–1–AAC 20–21. DOI: 10.1029/2002jd002128.

Rymer, H., B. van Wyk de Vries, J. Stix, and G. Williams-Jones (1998). "Pit crater structure and processes governing persistent activity at Masaya Volcano, Nicaragua". *Bulletin of Volcanology* 59(5), pp. 345–355. DOI: 10.1007/s004450050196.

Saxena, P. and C. Seigneur (1987). "On the oxidation of SO_2 to sulfate in atmospheric aerosols". *Atmospheric Environment (1967)* 21(4), pp. 807–812. DOI: 10.1016/0004-6981(87)90077-1.

Sayahi, T., A. Butterfield, and K. E. Kelly (2019). "Long-term field evaluation of the Plantower PMS low-cost particulate matter sensors". *Environmental Pollution* 245, pp. 932–940. DOI: 10.1016/j.envpol.2018.11.065.

Schlesinger, R. B. (1985). "Effects of inhaled acids on respiratory tract defense mechanisms." *Environmental Health Perspectives* 63, pp. 25–38. DOI: 10.1289/ehp.856325.

Schlesinger, R. B., N. Kunzli, G. M. Hidy, T. Gotschi, and M. Jerrett (2006). "The Health Relevance of Ambient Particulate Matter Characteristics: Coherence of Toxicological and Epidemiological Inferences". *Inhalation Toxicology* 18(2), pp. 95–125. DOI: 10.1080/08958370500306016.

Schmidt, A., S. Leadbetter, N. Theys, E. Carboni, C. S. Witham, J. A. Stevenson, C. E. Birch, T. Thordarson, S. Turnock, S. Barsotti, L. Delaney, W. Feng, R. G. Grainger, M. C. Hort, Á. Höskuldsson, I. Ialongo, E. Ilyinskaya, T. Jóhannsson, P. Kenny, T. A. Mather, N. A. D. Richards, and J. Shepherd (2015). "Satellite detection, long-range transport, and air quality impacts of volcanic sulfur dioxide from the 2014–2015 flood lava eruption at Bárðarbunga (Iceland)". *Journal of Geophysical Research: Atmospheres* 120(18), pp. 9739–9757. DOI: 10.1002/2015jd023638.

Shehab, M. A. and F. D. Pope (2019). "Effects of short-term exposure to particulate matter air pollution on cognitive performance". *Scientific Reports* 9(1). DOI: 10.1038/s41598-019-44561-0.

Shinohara, H., A. Aiuppa, G. Giudice, S. Gurrieri, and M. Liuzzo (2008). "Variation of H_2O/CO_2 and CO_2/SO_2 ratios of volcanic gases discharged by continuous degassing of Mount Etna volcano, Italy". *Journal of Geophysical Research* 113(B9). DOI: 10.1029/2007jb005185.

Sousan, S., K. Koehler, L. Hallett, and T. M. Peters (2016a). "Evaluation of the Alphasense optical particle counter (OPC-N2) and the Grimm portable aerosol spectrometer (PAS-1.108)". *Aerosol Science and Technology* 50(12), pp. 1352–1365. DOI: 10.1080/02786826.2016.1232859.

Sousan, S., K. Koehler, G. Thomas, J. H. Park, M. Hillman, A. Halterman, and T. M. Peters (2016b). "Inter-comparison of low-cost sensors for measuring the mass concentration of occupational aerosols". *Aerosol Science and Technology* 50(5), pp. 462–473. DOI: 10.1080/02786826.2016.1162901.

Stockwell, W. R. and J. G. Calvert (1983). "The mechanism of the HO-SO_2 reaction". *Atmospheric Environment (1967)* 17(11), pp. 2231–2235. DOI: 10.1016/0004-6981(83)90220-2.

Stoiber, R. E., S. N. Williams, and B. J. Huebert (1986). "Sulfur and halogen gases at Masaya Caldera Complex, Nicaragua: Total flux and variations with time". *Journal of Geophysical Research: Solid Earth* 91(B12), pp. 12215–12231. DOI: 10.1029/jb091ib12p12215.

Tam, E., R. Miike, S. Labrenz, A. J. Sutton, T. Elias, J. Davis, Y.-L. Chen, K. Tantisira, D. Dockery, and E. Avol (2016). "Volcanic air pollution over the Island of Hawai'i: Emissions, dispersal, and composition. Association with respiratory symptoms and lung function in Hawai'i Island school children". *Environment International* 92-93, pp. 543–552. DOI: 10.1016/j.envint.2016.03.025.

Tamburello, G. (2015). "Ratiocalc: Software for processing data from multicomponent volcanic gas analyzers". *Computers & Geosciences* 82, pp. 63–67. DOI: 10.1016/j.cageo.2015.05.004.

The Centre for Research Information (CRI) (2004). "Health effects of project SHAD chemical agent: Sulfur Dioxide". [CAS#: 7446-09-5].

Thermo Scientific (2010). *Model 43i sulphur dioxide analyser - product specifications*. URL: https://www.thermofisher.com/order/catalog/product/43I#/43I (visited on 01/10/2022).

Van Manen, S. M. (2014). "Perception of a chronic volcanic hazard: persistent degassing at Masaya volcano, Nicaragua". *Journal of Applied Volcanology* 3(1). doi: 10.1186/s13617-014-0009-3.

von Glasow, R., N. Bobrowski, and C. Kern (2009). "The effects of volcanic eruptions on atmospheric chemistry". *Chemical Geology* 263(1-4), pp. 131–142. doi: 10.1016/j.chemgeo.2008.08.020.

Whitty, R. C. W., E. Ilyinskaya, E. Mason, P. E. Wieser, E. J. Liu, A. Schmidt, T. Roberts, M. A. Pfeffer, B. Brooks, T. A. Mather, M. Edmonds, T. Elias, D. J. Schneider, C. Oppenheimer, A. Dybwad, P. A. Nadeau, and C. Kern (2020). "Spatial and Temporal Variations in SO_2 and PM2.5 Levels Around Kīlauea Volcano, Hawai'i During 2007–2018". *Frontiers in Earth Science* 8. doi: 10.3389/feart.2020.00036.

Williams-Jones, G. and H. Rymer (2015). "Hazards of Volcanic Gases". *The Encyclopedia of Volcanoes* 2, pp. 985–992. doi: 10.1016/B978-0-12-385938-9.00057-2.

Williams-Jones, G., H. Rymer, and D. A. Rothery (2003). "Gravity changes and passive SO_2 degassing at the Masaya caldera complex, Nicaragua". *Journal of Volcanology and Geothermal Research* 123(1-2), pp. 137–160. doi: 10.1016/s0377-0273(03)00033-7.